Available online at http://scik.org
Commun. Math. Biol. Neurosci. 2023, 2023:93
https://doi.org/10.28919/cmbn/8099
ISSN: 2052-2541

UNDERSTANDING THE INFLUENCE OF PREY ODOUR IN PREDATOR SPECIES: A THREE-SPECIES FOOD CHAIN STUDY

DEBASISH BHATTACHARJEE[1], DIPAM DAS[1], DIGANTA JYOTI SARMA[2], SANTANU ACHARJEE[1,*]

[1]Department of Mathematics, Gauhati University, Guwahati, Assam 781014, India

[2]Central Institute of Technology, Kokrajhar, Assam 783370, India

Abstract. The odour emitted by prey is typically regarded as a crucial factor in an ecosystem. The objective of this study is to examine the stability and local bifurcations, specifically transcritical and Hopf bifurcation, of a food chain model that takes into account the influence of odour. The proposed model has been developed by incorporating a three-species food chain and an additional factor that is more representative of reality: the impact of prey odour on predator population and, consequently, on the food chain. The system's solutions have been verified for positivity and boundedness. Subsequently, the conditions pertaining to the local stability and global stability of the equilibrium points of the proposed system, have been established. Additionally, the criteria for the emergence of bifurcations at certain equilibrium points are laid out. It has been observed that the equilibrium state of coexistence becomes unstable in the event of the absence of prey odour. The odour effect has been noted to play a role in promoting the coexistence of species within the food chain system, facilitated by the occurrence of two supercritical Hopf bifurcations. Furthermore, a comprehensive analysis of the impact of other different parameters within the system is presented. Subsequently, all the theoretical findings of this study are verified through a numerical analysis and outcomes are visually exhibited. The biological implications of the results are discussed and a conclusion has been drawn.

Keywords: predator-prey; food chain; odour effect; stability; bifurcation.

2020 AMS Subject Classification: 92B05, 92D40, 92D25, 34D20, 34D23, 34C23, 34C25.

*Corresponding author

E-mail address: sacharjee326@gmail.com

Received July 08, 2023

1. INTRODUCTION

The preservation of ecological balance within the ecosystem has become a major challenge for humanity throughout time. Consequently, the significance of investigating a dynamic system, particularly an ecological system, is on the rise. An ecological system is a conceptual representation of a trophic chain that depicts the interrelated relationships between predators and prey. In the discipline of ecology, food chains are comprised of a sequential succession of species that function to supply sustenance to the species located in close proximity to them. The analysis of a predator-prey model in mathematics involves the development of a mathematical model aimed at addressing fundamental ecological issues related to food chains. The mathematical model proposed by Lotka [1] and Volterra [2], which was first introduced in the literature, has undergone subsequent modifications to effectively represent the dynamics of predator-prey populations. The aforementioned alterations encompass the integration of pragmatic elements such as sophisticated functional responses [3,4], time delay [5,6], stage structure [7,8], hunting cooperation [9, 10], and fear effect [11, 12]. The present study examines a food chain model comprising three distinct species, namely the prey, middle predator, and top predator.

The functional response plays a crucial role in the prey-predator model by defining the nature of the interaction between the predator and prey. Therefore, the integration of appropriate functional responses into the prey-predator model formulation is a critical component of the modelling procedure. Numerous scholars have undertaken investigations into a range of predator-prey models, considering diverse categories of functional responses, including but not limited to Holling type I-IV, Beddington-De-Angelis type, Crowley-Martin type, and Ratio-dependent. The research conducted by Bhattacharjee et al. [13] pertained to an investigation of a model featuring two predators and one prey, utilising a Holling type I functional response. Majumdar et al. [14] conducted a study on a model of prey-predator interaction that incorporates a Holling type-II functional response. The utilisation of the Holling type III functional response has been observed in a model consisting of two predators and one prey, as presented by Didiharyono [15]. In addition, several other scholars [16–19] have investigated diverse models employing different functional responses.

Numerous studies have been conducted in scientific literature pertaining to various predator-prey interactions to date. The primary aspect of predator-prey dynamics that forms the basis of their interaction is the mechanism through which the predator and prey identify each other, even prior to any actual encounter. One of the noteworthy and significant interactions between predators and prey pertains to the response of predators to the odour of their prey. It is widely acknowledged [20] that individuals generate unique odours due to various factors such as metabolic activities, hormonal changes, etc. . In most cases, such odours are inadvertently released into the environment [20, 21]. The sense of odour can facilitate the differentiation and recognition of conspecifics and heterospecifics across various mammalian species. For instance, urinary scent marks are employed by mice as a means of communication with other members of their species in various social situations [21–23]. It has been established [20] that predators are attracted to the odours released by their prey. For example, blue crabs (Callinectes sapidus) have been observed to track prey odour plumes during their foraging activities [24]. According to studies [25], predators use informative cues like odours to efficiently locate and pursue potential prey. For instance, insectivorous avian species have the ability to utilise the chemical signals released by female moths, known as pheromones, to lure male moths as a means of detecting and capturing prey [26]. Canis lupus, commonly known as wolves, utilise olfactory cues to facilitate their hunting behaviour [27]. Also, the accumulation of odours resulting from roosting behaviour has the potential to attract predators and subsequently elevate the risk of predation [28]. Foxes exhibit an attraction to olfactory cues emitted by their prey [29]. Hence, the significance of odour is notably crucial. While the influence of prey odour on the process of predation is widely recognised in scholarly literature, there has been limited investigation into this subject matter within the context of a food chain. The impact of shelter on prey population in the presence of predator odour disturbance was examined by Shen et al. [30]. Also, Xu et al. [31] presented a model of predator-prey dynamics that incorporates the effects of odour disturbance and group defence. To the best of the authors' knowledge, these two articles are the sole works that examine the impact of odour that is relevant to our paper. So, there is a lack of literature in this area. To address this specific issue, the present work examines a food chain model comprising of three species while taking into consideration the impact of prey odour on

the food chain. The study incorporates a linear function response to model the consumption of prey by the middle predator, and a Holling type II functional response to model the consumption of middle predator, by the top predator.

The present manuscript is structured in the following manner: The fundamental description of the mathematical model is presented in Section 3. Section 4 of the paper examines the boundedness of solutions and the presence of a positive equilibrium point. In Section 5, the discussion pertaining to the existence of equilibrium points and their local stability has been undertaken. The global stability of the equilibrium points is addressed in Section 6. Bifurcation analysis is done in Section 7. In Section 8, the dynamic behaviour of the considered model has been discussed through graphical representations of its numerical findings. Section 9 concludes this paper by summarising its key findings and contributions.

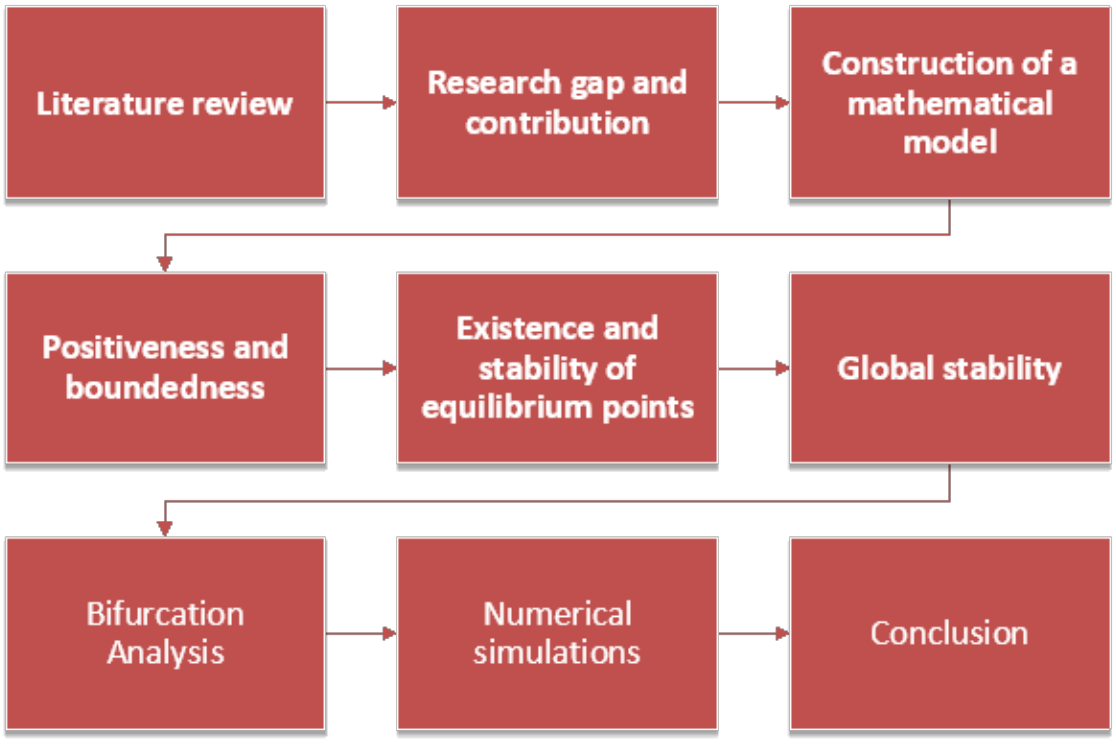

FIGURE 1. *A graphical representation of the research methodology utilised for the proposed model in the form of a flow chart.*

2. RESEARCH GAP AND CONTRIBUTION

Following a concise review of literature pertaining to food chain models in ecology, it is noted that a majority of researchers focused on various different effects such as fear effect, prey refuge, hunting cooperation by predators, etc that serve as extensions of the Lokta-Volterra model. Nonetheless, the extant literature exhibits certain absences, which are itemised as follows:

(a) The literature currently lacks sufficient investigation into the influence of odour on a three-species model consisting of a solitary prey and two predators.

(b) Several studies [30, 31] have explored the adverse impact of predator odour on prey, yet to date, no research has examined the potential positive effects of prey odour on predator populations, as far as the authors are aware.

In order to address the aforementioned gaps, our proposed three-species food chain model incorporates odour effect. In this paper, we have presented the olfactory impact as a detrimental factor for the prey and a beneficial factor for the predator. We consider prey odour aids predators in capturing their prey. Utilising this depiction, comprehensive theoretical and numerical evaluations pertaining to the stability and bifurcation of equilibrium points within the model have been conducted. Figure (1) depicts the research methodology utilised in the proposed model.

3. MATHEMATICAL MODELLING

In this section, a mathematical model is formulated to illustrate the influence of odour on a food chain system comprising three species. A system of three ordinary differential equations is utilised to depict the population dynamics of the prey, middle predator, and top predator, as well as their predation interactions. The mathematical formulation of the aforementioned biosystem commences with the conventional three-species food chain structure, followed by a gradual integration of the impact of prey odour on the intermediate predator (middle predator) within the food chain structure. The general form of a classical three-species food chain system is as follows.

$$\begin{aligned} \frac{ds}{dt} &= bs - ds - cs^2 - f_1(s)p_1 \\ \frac{dp_1}{dt} &= a_1 f_1(s)p_1 - f_2(p_1)p_2 - d_1 p_1 \\ \frac{dp_2}{dt} &= a_2 f_2(p_1)p_2 - d_2 p_2 \end{aligned} \tag{1}$$

The respective population sizes of the prey, middle predator, and top predator at a given time t are represented by the notations $s(t)$, $p_1(t)$, and $p_2(t)$. The variable b is utilised to denote the birth rate of the prey, whereas the intra-species competition coefficient of the prey is represented by c. The mortalities that occur naturally within the populations of the prey, middle predator, and top predator are denoted by d, d_1, and d_2, respectively. The respective conversion efficiencies of the middle predator and top predator are denoted as a_1 and a_2. Additionally, it can be noted that $f_1(s)$ and $f_2(p_1)$ represent the functional responses of the middle predator and the apex predator, respectively, in relation to their prey.

The release of olfactory cues by prey can play a pivotal role in facilitating the predatory behaviour of predators, thereby assisting in the identification and capture of their prey [32]. For instance, coyote (Canis latrans) [32] and bears [33,34], etc. exhibit a highly developed olfactory system that allows them to perceive potential food from a distance, even in the absence of visual stimuli. This enhances their ability to effectively locate and pursue their target. Following these instances, it is clear that the role of prey odour in predation by the predators within a food chain is of significant importance, neglecting this factor in mathematical modelling may result in a less impactful model. So, in this study, the role of prey odour in facilitating efficient tracking and hunting by predators is taken into consideration. We hypothesise that prey odour aids in the predation process of the middle predator. We also assume that the quantity of odour released by prey has a direct correlation with prey population size. To account for this relationship, we incorporate the expression (1 + γ s) into the functional response of the middle predator with respect to its prey. Consequently, the model (1) incorporating the odour effect becomes

$$
\begin{aligned}
\frac{ds}{dt} &= r_1 s(1-s) - r_2(1+\gamma s)sp_1 \\
\frac{dp_1}{dt} &= r_3 r_2(1+\gamma s)sp_1 - \frac{r_4 p_1 p_2}{(1+bp_1)} - d_1 p_1 \\
\frac{dp_2}{dt} &= \frac{r_5 r_4 p_1 p_2}{(1+bp_1)} - d_2 p_2
\end{aligned} \tag{2}
$$

with initial conditions: $s(0) = s^0 > 0$, $p_1(0) = p_1^0 > 0$, and $p_2(0) = p_2^0 > 0$.

Here, the population sizes of the prey, middle predator, and top predator at a specific time t are denoted as $s(t)$, $p_1(t)$, and $p_2(t)$ respectively. The meanings of all other parameters relevant to the model (2) are delineated in table (1).

Parameter	Significance
r_1	Intrinsic growth rate of prey
r_2	Intake rate of middle predator to prey
r_3	Prey biomass conversion rate to middle predator biomass
r_4	Intake rate of top predator to middle predator
r_5	Middle predator biomass conversion rate to top predator biomass
b	Top predator handling time per prey (middle predator)
γ	coefficient of odor effect produced by a single prey.
d_1	Intrinsic mortality rate of the middle predator
d_2	Intrinsic mortality rate of the top predator

TABLE 1. *The biological implications of the parameters associated with system (2).*

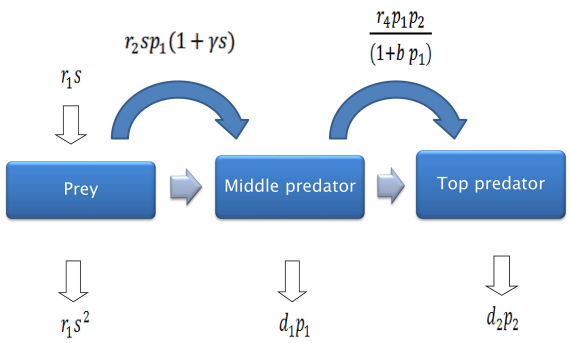

FIGURE 2. *The dynamical interactions of prey, middle-predator, and top-predator under the impact of prey odour are depicted in a schematic diagram.*

4. Positiveness and Boundedness

Positiveness: From system (2), after some calculations, we get

$$\text{s(t)=s(0) exp}\left[\int_0^t \Big(r_1(1-s(r))-r_2(1+\gamma s(r))p_1(r)\Big)\,dr\right],$$

$$p_1(t)=p_1(0)\text{exp}\left[\int_0^t \Big(r_3r_2(1+\gamma s(r))s(r)-\tfrac{r_4p_2(r)}{(1+bp_1(r))}-d_1\Big)\,dr\right], \text{ and}$$

$$p_2(t)=p_2(0)\text{exp}\left[\int_0^t \Big(\tfrac{r_5r_4p_1(r)}{(1+bp_1(r))}-d_2\Big)\,dr\right]$$

As $s(0)=s^0>0$, $p_1(0)=p_1^0>0$, $p_2(0)=p_2^0>0$ i.e., $s(t),p_1(t),p_2(t)>0,\forall t$. Thus, all the solutions of the system (2) are positive.

Boundedness: The population of prey is consistently restricted by an upper bound as $\frac{ds}{dt}\leq r_1s(1-s)$ which after integrating gives $\lim_{t\to\infty}s\leq 1$.

Now, we define $x=s+p_1+p_2$, and $\nu>0$ be an arbitary real number. Taking derivative w.r.t time 't' and using system (2), we get

$$\frac{dx}{dt}+\nu x\leq(r_1+\nu)s-(d_1-\nu)p_1-(d_2-\nu)p_2$$

Now, we choose $\nu\leq min(d_1,d_2)$ and W is some constant, then

$$(r_1+\nu)s-(d_1-\nu)p_1-(d_2-\nu)p_2\leq(r_1+\nu)s\leq(r_1+\nu)=W$$

. Now, we employ conventional results on differential inequalities and taking V is some constant

$$x(t)\leq\frac{W}{\nu}+\big(x(0)-\frac{W}{\nu}\big)e^{-\nu t}\leq max\big((x(0),\frac{W}{\nu}\big)=V$$

Hence, it can be deduced that there is a positive value V, which solely relies on the parameters of system (2), such that $0<w(t)\leq V$ for values of t that are considerably large. Therefore, it can be concluded that all populations within the system are ultimately limited by upper bounds.

5. Equilibrium Points and Their Stability

5.1. Existence of equilibrium points. In order to calculate the fixed points of the system (2), we solve the following simultaneous equations:

$$
\begin{aligned}
& r_1 s(1-s) - r_2(1+\gamma s)sp_1 = 0 \\
& r_3 r_2(1+\gamma s)sp_1 - \frac{r_4 p_1 p_2}{(1+bp_1)} - d_1 p_1 = 0 \\
& \frac{r_5 r_4 p_1 p_2}{(1+bp_1)} - d_2 p_2 = 0
\end{aligned} \tag{3}
$$

Upon performing calculations, it has been found that model (2) exhibits five equilibrium points that are non-negative in nature. These points are namely, extinction equilibrium $E_0 = (0,0,0)$, prey only equilibrium $E_1 = (1,0,0)$, boundary equilibrium point $E_2 = (A_1, B_1, 0)$ and the most important interior equilibria $E^{'} = (s^{'}, p_1^{'}, p_2^{'})$.

Here,

$$A_1 = -\frac{1}{2\gamma} + \frac{\sqrt{4d_1\gamma + r_2 r_3}}{2\gamma\sqrt{r_2 r_3}}, B_1 = -\frac{r_1(2d_1\gamma + (1+\gamma)\sqrt{r_2 r_3}(-\sqrt{r_2 r_3} - \sqrt{4d_1\gamma + r_2 r_3}))}{2d_1\gamma^2 r_2},$$

$$s^{'} = \frac{bd_2 r_1 + d_2 r_2 - r_1 r_4 r_5}{bd_2 r_1 - d_2\gamma r_2 - r_1 r_4 r_5}, p_1^{'} = -\frac{d_2}{bd_2 - r_4 r_5}, p_2^{'} = \frac{\beta_1}{(bd_2 - r_4 r_5)(-bd_2 r_1 + d_2\gamma r_2 + r_1 r_4 r_5)^2}$$

and $\beta_1 = r_5(b^2 d_2^2 r_1^2(d_1 - (1+\gamma)r_2 r_3) + (1+\gamma)r_1 r_2 r_3 r_4 r_5(d_2 r_2 - r_1 r_4 r_5) + d_1(d_2\gamma r_2 + r_1 r_4 r_5)^2 - bd_2 r_1((1+\gamma)r_2 r_3(d_2 r_2 - 2r_1 r_4 r_5) + 2d_1(d_2\gamma r_2 + r_1 r_4 r_5)))$.

The existence conditions of these equilibrium points are as follows:

(1) E_0 and E_1 always exists.

(2) E_2 exists if $r_2 r_3 > \frac{d_1}{1+\gamma}$.

(3) $E^{'}$ exists if $r_1 > -\frac{(d_2 r_2)}{(bd_2 - r_4 r_5)}$, $r_3 > \frac{\beta_2}{\beta_3}$ and $b < \frac{r_4 r_5}{d_2}$.
Here, $\beta_2 = b^2 d_1 d_2^2 r_1^2 - 2bd_1 d_2^2\gamma r_1 r_2 + d_1 d_2^2\gamma^2 r_2^2 - 2bd_1 d_2 r_1^2 r_4 r_5 + 2d_1 d_2\gamma r_1 r_2 r_4 r_5 + d_1 r_1^2 r_4^2 r_5^2$, $\beta_3 = b^2 d_2^2 r_1^2 r_2 + b^2 d_2^2\gamma r_1^2 r_2 + bd_2^2 r_1 r_2^2 + bd_2^2\gamma r_1 r_2^2 - 2bd_2 r_1^2 r_2 r_4 r_5 - 2bd_2\gamma r_1^2 r_2 r_4 r_5 - d_2 r_1 r_2^2 r_4 r_5 - d_2\gamma r_1 r_2^2 r_4 r_5 + r_1^2 r_2 r_4^2 r_5^2 + \gamma r_1^2 r_2 r_4^2 r_5^2$.

5.2. Local stability. This section pertains to the examination of the local stability of the system (2) with the utilisation of the eigenvalue analysis approach, with regard to all equilibrium points. In order to assess the local stability of the equilibrium points of system (2), it is necessary to derive the Jacobian matrix at each equilibrium point. The Jacobian matrix at a point (s, p_1, p_2) is given by

$$J_{(s,p_1,p_2)} = \begin{bmatrix} r_1 - 2r_1 s - p_1 r_2(1+2\gamma s) & -r_2 s(1+\gamma s) & 0 \\ p_1 r_2 r_3(1+2\gamma s) & -d_1 + \frac{-p_2 r_4 + (1+bp_1)^2 r_2 r_3 s(1+\gamma s)}{(1+bp_1)^2} & -\frac{p_1 r_4}{1+bp_1} \\ 0 & \frac{p_2 r_4 r_5}{(1+bp_1)^2} & -d_2 + \frac{p_1 r_4 r_5}{1+bp_1} \end{bmatrix}$$

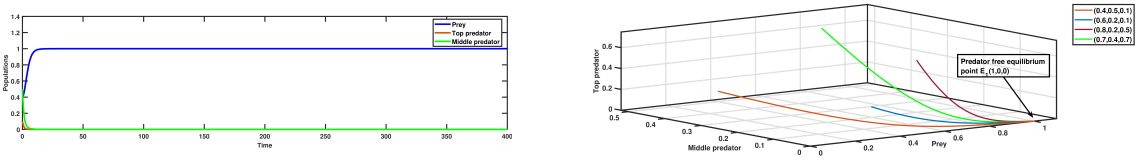

(A) *Local stability* (B) *Global stability*

FIGURE 3. *Local and global stability of the axial equilibrium point* E_1.

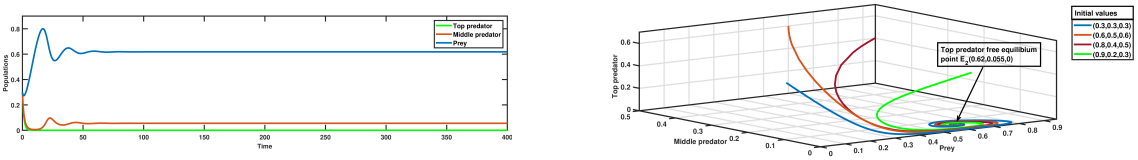

(A) *Time series* (B) *Phase portrait*

FIGURE 4. *Local stability of the boundary equilibrium point* E_2.

The following theorem pertains to the local stability of the equilibria of system (2).

Theorem 1. *(1) The population free equilibrium point* E_0 *is unstable.*

(2) The axial equilibrium point E_1 *is asymptotically stable if* $r_2 r_3 < \frac{d_1}{1+\gamma}$.

(3) The top predator free equilibrium point E_2 *is locally stable if* $K_i > 0$*, i=1, 2, 3 and* $K_1 K_2 > K_3$*. The meanings of the symbols* K_i *are given within the proof.*

(4) The interior equilibrium point $E^{'}$ *is asymptotically stable if* $L_i > 0$*, i=1, 2, 3 and* $L_1 L_2 > L_3$*. The meanings of the symbols* L_i *are given within the proof.*

Proof. (1) The eigenvalues of the Jacobian matrix of the system (2) at E_0 are r_1 , -d_1 and -d_2. As, the eigenvalues are of opposite signs which indicates E_0, i.e., the population free equilibrium point is a saddle point, i.e., unstable.

(2) The Jacobian matrix of the system (2) at E_1 is

$$J_{(1,0,0)} = \begin{bmatrix} -r_1 & -(1+\gamma)r_2 & 0 \\ 0 & -d_1+(1+\gamma)r_2r_3 & 0 \\ 0 & 0 & -d_2 \end{bmatrix}$$

Hence, the eigenvalues are $-r_1$, $-d_1+(1+\gamma)r_2r_3$, and $-d_2$. The eigenvalue $-d_1+(1+\gamma)r_2r_3$ is negative if $r_2r_3 < \frac{d_1}{1+\gamma}$. As a result, E_1 is locally stable if these conditions hold.

(3) For the equilibrium point E_2, the Jacobian matrix is

$$J_{(A_1,B_1,0)} = \begin{bmatrix} p_{11} & p_{12} & 0 \\ p_{21} & 0 & p_{23} \\ 0 & 0 & p_{33} \end{bmatrix}$$

Here,

$$p_{11} = -\frac{(1+\gamma)r_1(2d_1\gamma+r_2r_3-\sqrt{r_2r_3}\sqrt{4d_1\gamma+r_2r_3})}{(2d_1\gamma^2)}, p_{12} = -\frac{d1}{r3},$$

$$p_{21} = \frac{r_1\sqrt{r_3}\sqrt{4d_1\gamma+r_2r_3}(-2d_1\gamma+(1+\gamma)\sqrt{r_2r_3}(-\sqrt{r_2r_3}+\sqrt{4d_1\gamma+r_2r_3}))}{2d_1\gamma^2\sqrt{r_2}},$$

$$p_{23} = \frac{r_1(2d_1\gamma+(1+\gamma)\sqrt{r_2r_3}(\sqrt{r_2r_3}-\sqrt{4d_1\gamma+r_2r_3}))r_4}{2d_1\gamma^2r_2+br_1(-2d_1\gamma+(1+\gamma)\sqrt{r_2r_3}(-\sqrt{r_2r_3}+\sqrt{4d_1\gamma+r_2r_3}))},$$

$$p_{33} = -d_2+\frac{r_1(2d_1\gamma-(1+\gamma)\sqrt{r_2r_3}(\sqrt{r_2r_3}-\sqrt{4d_1\gamma+r_2r_3}))r_4r_5}{-2d_1\gamma^2r_2+br_1(2d_1\gamma+(1+\gamma)\sqrt{r_2r_3}(\sqrt{r_2r_3}-\sqrt{4d_1\gamma+r_2r_3}))}$$

Let us consider, $\delta_1^3+K_1\delta_1^2+K_2\delta_1+K_3=0$, be the characteristic equation of $J_{(A_1,B_1,0)}$. Here, $K_1=-(p_{11}+p_{33})$, $K_2=-(p_{12}p_{21}-p_{11}p_{33})$, and $K_3=p_{12}p_{21}p_{33}$. By Routh-Hurwitz criterion, the top predator free equilibrium is locally asymptotically stable provided $K_i>0$, i=1, 2, 3 and $K_1K_2>K_3$.

(4) The variational matrix at the coexistent equilibrium point $E^{'}$ is given by

$$J_{(s',p_1',p_2')} == \begin{bmatrix} q_{11} & q_{12} & 0 \\ q_{21} & q_{22} & p_{23} \\ 0 & q_{32} & 0 \end{bmatrix}$$

Here,

$$q_{11} = -\frac{bd_2r_1 + d_2r_2 - r_1r_4r_5}{bd_2 - r_4r_5}, q_{12} = -\frac{(1+\gamma)r_1r_2(bd_2 - r_4r_5)(bd_2r_1 + d_2r_2 - r_1r_4r_5)}{(-bd_2r_1 + d_2\gamma r_2 + r_1r_4r_5)^2},$$

$$q_{21} = -\frac{d_2r_2r_3(bd_2(1+2\gamma)r_1 + d_2\gamma r_2 - (1+2\gamma)r_1r_4r_5)}{(bd_2 - r_4r_5)(bd_2r_1 - d_2\gamma r_2 - r_1r_4r_5)}, q_{22} = \frac{\rho_1}{r_4r_5(-bd_2r_1 + d_2\gamma r_2 + r_1r_4r_5)^2},$$

$$q_{23} = -\frac{d_2}{r_5}, q_{32} = \frac{\rho_2}{r_4(-bd_2r_1 + d_2\gamma r_2 + r_1r_4r_5)^2}.$$

where,

$\rho_1 = bd_2(b^2d_2^2r_1^2(-d_1 + r_2r_3(1+\gamma) + (1+\gamma)r_1r_2r_3r_4r_5(-d_2r_2 + r_1r_4r_5) - d_1(d_2\gamma r_2 + r_1r_4r_5)^2 + bd_2r_1((1+\gamma)r_2r_3(d_2r_2 - 2r_1r_4r_5) + 2d_1(d_2\gamma r_2 + r_1r_4r_5))),$

$\rho_2 = (-bd_2 + r_4r_5)(b^2d_2^2r_1^2(-d_1 + (1+\gamma)r_2r_3) + (1+\gamma)r_1r_2r_3r_4r_5(-d_2r_2 + r_1r_5) - d_1(d_2\gamma r_2 + r_1r_4r_5)^2 - bd_2r_1((1+\gamma)r_2r_3(d_2r_2 - 2r_1r_4r_5) + 2d_1(d_2\gamma r_2 + r_1r_4r_5)))$

Let, the characteristic equation of $J_{(s',p_1',p_2')}$ is given by

$$\delta_2^3 + L_1\delta_2^2 + L_2\delta_2 + L_3 = 0 \tag{4}$$

Here, $L_1 = -(q_{11} + q_{22})$, $L_2 = (-q_{12}q_{21} + q_{11}q_{22} - q_{23}q_{32})$, and $L_3 = q_{11}q_{23}q_{32}$. Using Routh-Hurwitz criterion, the coexistent equilibrium point E' is locally asymptotically stable if the conditions $L_i > 0$, i=1, 2, 3 and $L_1L_2 > L_3$ hold simultaneously.

□

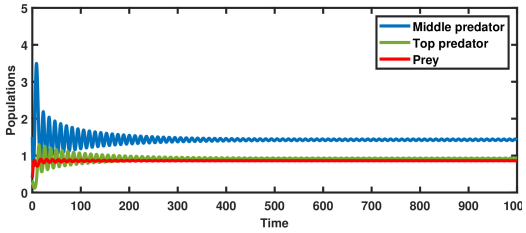

(A) *Local stability*

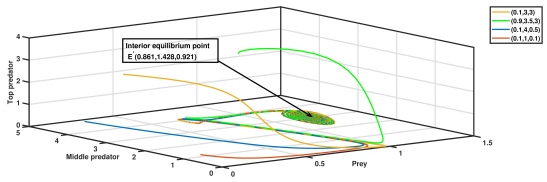

(B) *Global stability*

FIGURE 5. *Local and global stability of the interior equilibrium point* E'.

6. GLOBAL STABILITY

The analysis of local stability pertains to the study of the system's behaviour in the immediate proximity of the equilibrium point. On the contrary, global stability analysis pertains to the examination of the system's behaviour across its entire state space, encompassing not only the vicinity of the equilibrium point. The inquiry pertains to the examination of the convergence of all trajectories, irrespective of their initial conditions, towards the equilibrium point as time progresses. Some related theorems are listed below.

Theorem 2. *The global asymptotic stability of the axial equilibrium E_1 is contingent upon the fulfilment of the condition $r_2 r_3 < \frac{d_1}{1+\gamma}$.*

Proof. The Jacobian matrix of the system (2) at the equilibrium point E_1 is $J_{(1,0,0)}$ which is given by

$$J_{(1,0,0)} = \begin{bmatrix} -r_1 & -(1+\gamma)r_2 & 0 \\ 0 & -d_1+(1+\gamma)r_2 r_3 & 0 \\ 0 & 0 & -d_2 \end{bmatrix}$$

Now, the equilibrium point E_1 is asymptotically stable if $-d_1+(1+\gamma)r_2 r_3 < 0$ as stated in the previous section. From system (2), we have

$$\begin{aligned} \frac{dp_1}{dt} &= r_3 r_2 (1+\gamma s) s p_1 - \frac{r_4 p_1 p_2}{(1+bp_1)} - d_1 p_1 \\ &< ((1+\gamma s) r_2 r_3 - d_1) p_1 \end{aligned}$$

As per the comparison theorem, $p_1(t) \to 0$ as $t \to \infty$ if $(1+\gamma s) r_2 r_3 - d_1 < 0$ holds. Additionally, it can be observed that $p_2(t)$ approaches to zero as $p_1(t)$ approaches to zero. Drawing from the theoretical framework of asymptotical autonomous systems as outlined in [35], system (2) can be simplified to a limiting system

$$\frac{ds}{dt} = r_1 s(1-s)$$

This suggests that the function $s(t)$ approaches to 1. This implies that the equilibrium point E_1 exhibits global attractivity. Consequently, it can be concluded that the system denoted by E_1 exhibits global asymptotic stability. □

Theorem 3. *Global asymptotic stability of the interior equilibrium point $E^{'}$ is ensured under the fulfilment of the specified conditions:(a)* $\vartheta_1 > \frac{s^{'}p_1^{'}\theta_2+s^{'}p_1^{'}r_3\theta_2+s^{'}\vartheta_2\theta_2+r3\vartheta_2\theta_2^2}{\theta_1^2}$, *(b)* $r_3 < 1$, *(c)* $r_5 < 1$, *(d)* $\gamma < \frac{1-r_3}{s^{'}r_3}$, *and (e)* $r_2 > \frac{-p_2^{'}r_4\vartheta_2-p_1^{'}r_4\Theta_2}{-\gamma\vartheta_1\theta_1^2+s^{'}p_1^{'}\gamma\theta_2+s^{'}p_1^{'}r_3\gamma\theta_2+s^{'}\gamma\vartheta_2\theta_2+\gamma r_3\vartheta_2\theta_2^2}$.

Proof. The establishment of the global stability of the interior equilibrium $E^{'}$ can be achieved through the construction of a Lyapunov function W, which is constructed in the following manner

$$W = (s-s^{'}-s^{'}ln\frac{s}{s^{'}})+(p_1-p_1^{'}-p_1^{'}ln\frac{p_1}{p_1^{'}})+(p_2-p_2^{'}-p_2^{'}ln\frac{p_2}{p_2^{'}})$$

Hence, the time derivative of the aforementioned equation is

$$\frac{dW}{dt} = \frac{(s-s^{'})}{s}\frac{ds}{dt}+\frac{(p_1-p_1^{'})}{p_1}\frac{dp_1}{dt}+\frac{(p_2-p_2^{'})}{p_2}\frac{dp_2}{dt} = W_1+W_2+W_3$$

where, $W_1 = \frac{(s-s^{'})}{s}\frac{ds}{dt}$, $W_2 = \frac{(p_1-p_1^{'})}{p_1}\frac{dp_1}{dt}$, and $W_3 = \frac{(p_2-p_2^{'})}{p_2}\frac{dp_2}{dt}$. Using equations of system (2), we get

$$\begin{aligned} W_1 &= -r_1(s-s^{'})^2 - r_2(s-s^{'})(p_1-p_1^{'}) - r_2\gamma(s-s^{'})(sp_1-s^{'}p_1^{'}) \\ W_2 &= r_3r_2(p_1-p_1^{'})(s-s^{'})+r_3r_2\gamma(s^2-s^{'2})+(p_1-p_1^{'})+r_4\kappa \\ W_3 &= r_5r_4(p_2-p_2^{'})(\frac{p_1}{1+bp_1}-\frac{p_1^{'}}{1+bp_1^{'}}) \end{aligned} \tag{5}$$

where, $\kappa = (p_1-p_1^{'})(\frac{p_2^{'}}{1+bp_1^{'}}-\frac{p_2}{1+bp_1})$. Upon performing some calculations to simplify W_1, W_2, and W_3, we get

$W_1+W_2+W_3 = -r_1(s-s^{'})^2 - r_2\gamma(s-s^{'})(sp_1-s^{'}p_1^{'}) + (s-s^{'})(p_1-p_1^{'})(-r_2+r_3r_2+r_3r_2\gamma s^{'})+(s-s^{'})(p_1-p_1^{'})r_3r_2\gamma s+\frac{p_1p_2(-r_4+r_5r_4))}{1+bp_1}+\frac{r_4p_1^{'}p_2}{1+bp_1}-\frac{r_5r_4p_1p_2^{'}}{1+bp_1}+\frac{p_1^{'}p_2^{'}(-r_4+r_5r_4))}{1+bp_1^{'}}+\frac{r_4p_2^{'}p_1}{1+bp_1^{'}}-\frac{r_5r_4p_2p_1^{'}}{1+bp_1^{'}}$

Now, we may assume $\theta_1 \le s \le \theta_2$, $\vartheta_1 \le p_1 \le \vartheta_2$, and $\Theta_1 \le p_2 \le \Theta_2$ and thus we get

$$W_1+W_2+W_3 \le -r_2\gamma(s-s^{'})(sp_1-s^{'}p_1^{'})+(s-s^{'})(p_1-p_1^{'})(-r_2+r_3r_2+r_3r_2\gamma s^{'})$$
$$+(s-s^{'})(p_1-p_1^{'})r_3r_2\gamma s+\frac{p_1p_2(-r_4+r_5r_4))}{1+bp_1}+\frac{r_4p_1^{'}p_2}{1+bp_1}+\frac{p_1^{'}p_2^{'}(-r_4+r_5r_4))}{1+bp_1^{'}}+\frac{r_4p_2^{'}p_1}{1+bp_1^{'}}$$

Now, $W_1+W_2+W_3 < 0$ if the expression

$$r_4p_1^{'}\Theta_2+r_4p_2^{'}\vartheta_2+r_3r_2\gamma\theta_2^2\vartheta_2+r_3r_2\gamma\theta_2s^{'}p_1^{'}+r_2\gamma\theta_2s^{'}p_1^{'}+r_2\gamma s^{'}\theta_2\vartheta_2-r_2\gamma\theta_1^2\vartheta_1 < 0 \tag{6}$$

The abovementioned inequality (6) holds if the following criteria are met:
(a) $\vartheta_1 > \frac{s^{'}p_1^{'}\theta_2+s^{'}p_1^{'}r_3\theta_2+s^{'}\vartheta_2\theta_2+r3\vartheta_2\theta_2^2}{\theta_1^2}$, (b) $r_3 < 1$, (c) $r_5 < 1$, (d) $\gamma < \frac{1-r_3}{s^{'}r_3}$, and
(e) $r_2 > \frac{-p_2^{'}r_4\vartheta_2-p_1^{'}r_4\Theta_2}{-\gamma\vartheta_1\theta_1^2+s^{'}p_1^{'}\gamma\theta_2+s^{'}p_1^{'}r_3\gamma\theta_2+s^{'}\gamma\vartheta_2\theta_2+\gamma r_3\vartheta_2\theta_2^2}$.
Therefore, it can be concluded that $\frac{dW}{dt} < 0$, i.e., the interior equilibrium is globally stable provided that the conditions (a), (b), (c), (d), and (e) are satisfied. □

7. BIFURCATION ANALYSIS

The analysis of bifurcation is of paramount importance in comprehending intricate systems and forecasting their performance under varying circumstances. The study of bifurcations can offer valuable insights into the manner in which minor alterations in parameters can result in substantial alterations in the behaviour of a system.

7.1. Transcritical bifurcation. The transcritical bifurcation will be discussed in this section. The phenomenon of transcritical bifurcation is characterised by a significant alteration in the qualitative dynamics of a system, which occurs as a result of the exchange of stability properties between equilibrium points.

Theorem 4. *The system (2) yields a transcritical bifurcation at the critical parameter value* $\gamma = \frac{d_1-r_2r_3}{r_2r_3} = \gamma^{tc}$ *around the equilibrium point* E_1 *provided* $r_2r_3 \neq 0$.

Proof. The Jacobian matrix of the system (2) at the coexisting equilibrium point E_1 is $J_{(s^{'},p_1^{'},p_2^{'})}$ as previously stated in the preceding section. Taking $\gamma = \frac{d_1-r_2r_3}{r_2r_3} = \gamma^{tc}$, we get

$$J_{(s^{'},p_1^{'},p_2^{'})_{\gamma=\gamma^{tc}}} = \begin{bmatrix} -r_1 & -(1+\gamma)r_2 & 0 \\ 0 & 0 & 0 \\ 0 & 0 & -d_2 \end{bmatrix}$$

Now, let us consider two eigenvectors U and V, which correspond to the zero eigenvalue of $J_{(s^{'},p_1^{'},p_2^{'})_{\gamma=\gamma^{tc}}}$ and $J^T_{(s^{'},p_1^{'},p_2^{'})_{\gamma=\gamma^{tc}}}$, respectively. After some computation, we get $U = (u_1,u_2,u_3)^t = (-\frac{(r_2+\gamma r_2)}{r_1},1,0)^t$ and $V = (v_1,v_2,v_3)^t = (0,1,0)^t$. Now, Sotomayor's theorem [36] is employed to establish the existence of a transcritical bifurcation on the parametric surface $-d_1+(1+\gamma)r_2r_3$=0 in the vicinity of E_1. The prerequisites for transcritical

bifurcation as per Sotomayor's theorem are outlined as follows:

$$Z_\gamma(E_1;\gamma^{tb}) = \begin{bmatrix} 0 \\ 0 \\ 0 \end{bmatrix}, D(Z_\gamma(E_1;\gamma^{tb}))U = \begin{bmatrix} 0 & -r_2 & 0 \\ 0 & r_2 r_3 & 0 \\ 0 & 0 & 1 \end{bmatrix} \begin{bmatrix} -\frac{(r_2+\gamma r_2)}{r_1} \\ 1 \\ 0 \end{bmatrix} = \begin{bmatrix} -r_2 \\ r_2 r_3 \\ 0 \end{bmatrix}, \text{ and}$$

$$D^2(Z_\gamma(E_1;\gamma^{tb}))(U,U) = \begin{bmatrix} \frac{2\gamma(1+\gamma)r_2^2}{r_1} \\ -\frac{(2(1+\gamma)(1+2\gamma)r_2^2 r_3}{r_1} \\ 0 \end{bmatrix}.$$

Therefore,

$$V^T(Z_\gamma(E_1;\gamma^{tb})) = 0$$

$$V^T(D(Z_\gamma(E_1;\gamma^{tb}))U) = r_2 r_3 \neq 0,$$

$$V^T(D^2(Z_\gamma(E_1;\gamma^{tb}))(U,U)) = -\frac{(2(1+\gamma)(1+2\gamma)r_2^2 r_3}{r_1} \neq 0$$

Thus, the verification of a transcritical bifurcation in the vicinity of E_1 at $\gamma = \frac{d_1 - r_2 r_3}{r_2 r_3} = \gamma^{tc}$ is established utilising Sotomayor's theorem [36]. Alternatively, other parameters may also be utilised as bifurcating parameters. □

7.2. Hopf bifurcation. This subsection discusses the Hopf bifurcation. A Hopf bifurcation occurs when a system undergoes a significant change in stability, leading to the emergence of a periodic solution, at a specific critical value of a parameter. In this section, the Hopf bifurcation is examined in an analytical manner by investigating the coexistence equilibrium $E^{'}$ with regard to the parameter denoting the odour effect γ, while holding all other parameters constant. In the theorem presented below, we demonstrate the existence of a Hopf bifurcation by considering the parameter γ as the bifurcation parameter.

Theorem 5. *The system (2) undergoes Hopf bifurcation in the vicinity of the positive equilibrium $E^{'}$, when the parameter γ passes a critical value γ^H if and only if the following conditions are met:*

(a) $L_1(\gamma^H) > 0$ *, (b)* $L_3(\gamma^H) > 0$*, (c)* $L_1(\gamma^H)L_2(\gamma^H) = L_3(\gamma^H)$*, and (d)* $(L_1(\gamma^H)L_2(\gamma^H))^{'} \neq L_3^{'}(\gamma^H)$

Proof. The characteristic equation of the system (2) in the vicinity of coexisting equilibrium $E^{'}$ is given by the equation (4). When the parameter γ attains its critical value γ^H, i.e., $\gamma = \gamma^H$, then the equation (4) becomes

$$(\delta_2^2 + L_2)(\delta_2 + L_1) = 0 \tag{7}$$

The roots of the equation (7) are $\delta_1 = i\sqrt{L_2}$, $\delta_2 = -i\sqrt{L_2}$, and $\delta_3 = -L_1$. Now, in order to show the occurrence of Hopf bifurcation at $\gamma = \gamma^H$, it is necessary to fulfil the transversality condition $(\frac{d\delta_i}{d\gamma})_{\gamma=\gamma^H} \neq 0$, i=1, 2, 3. Let us consider, the roots are of the form

$$\delta_1(\gamma) = \chi_1(\gamma) + i\chi_2(\gamma),$$

$$\delta_2(\gamma) = \chi_1(\gamma) - i\chi_2(\gamma),$$

$$\delta_3(\gamma) = -L_1$$

Substituting the values of $\delta_i(\gamma)$, i=1, 2 in equation (7) and calculating the derivatives, we get

$$Q(\gamma)\chi_1^{'}(\gamma) - R(\gamma)\chi_2(\gamma) + S(\gamma) = 0,$$

$$R(\gamma)\chi_1^{'}(\gamma) + Q(\gamma)\chi_2(\gamma) + T(\gamma) = 0$$

where,

$$Q(\gamma) = 3\chi_1^2(\gamma) + 2L_1(\gamma)\chi_1(\gamma) + L_2(\gamma) - 3\chi_2^2(\gamma),$$

$$R(\gamma) = 6\chi_1(\gamma)\chi_2(\gamma) + 2L_1(\gamma)\chi_2(\gamma),$$

$$S(\gamma) = \chi_1^2(\gamma)L_1^{'}(\gamma) + L_2^{'}(\gamma)\chi_1(\gamma) + L_3^{'}(\gamma) - L_1^{'}(\gamma)\chi_2^2(\gamma),$$

$$T(\gamma) = 2\chi_1(\gamma)\chi_2(\gamma)L_1^{'}(\gamma) + L_2^{'}(\gamma)\chi_2(\gamma)$$

Since, $\chi_1(\gamma^H) = 0$, and $\chi_2(\gamma^H) = \sqrt{L_2(\gamma^H)}$, so we have

$$Q(\gamma^H) = -2L_2(\gamma^H), R(\gamma^H) = 2L_1(\gamma^H)\sqrt{L_2(\gamma^H)},$$

$$S(\gamma^H) = L_3^{'}(\gamma^H) - L_1^{'}(\gamma^H)L_2(\gamma^H), T(\gamma^H) = L_2^{'}(\gamma^H)\sqrt{L_2(\gamma^H)}$$

Therefore,

$$\frac{d}{d\gamma}(Re((\delta_i)(\gamma)))_{\gamma=\gamma^H} = -\frac{R(\gamma^H)T(\gamma^H) + Q(\gamma^H)S(\gamma^H)}{Q^2(\gamma^H) + R^2(\gamma^H)} \neq 0, i = 1,2$$

if $(L_1(\gamma^H)L_2(\gamma^H))' \neq L_3'(\gamma^H)$ and $\delta_3(\gamma^H) = -L_1 \neq 0$.

Consequently, the conditions of transversality are satisfied. This suggests that a Hopf bifurcation takes place when $\gamma = \gamma^H$. Therefore, the theorem holds true. Other parameters can also be considered as bifurcating parameters. □

7.3. Direction and stability of Hopf bifurcations.

Theorem 6. *[37] The direction of Hopf bifurcation can be elucidated by the sign of $\mu_2\alpha'(0)$. The biosystem (2) undergoes a supercritical Hopf bifurcation when the condition $\mu_2\alpha'(0) > 0$ is met, while a subcritical Hopf bifurcation occurs when $\mu_2\alpha'(0) < 0$. The bifurcating periodic solution's stability is indicated by β_2, whereby a negative value of β_2 indicates stability, while a positive value of β_2 indicates instability. Here, $\alpha'(0)$, μ_2, and β_2 are being used in their conventional sense.*

8. Numerical Simulations

The validation of analytical studies necessitates the numerical verification of the obtained outcomes. In this section, we explore the dynamics of system (2) quantitatively by selecting parameter values in biologically viable region. We present a computer simulation of various solutions of system (2) utilising MATLAB and MATCONT [38]. Unless stated otherwise, the numerical results presented in this study employ the parameter values outlined in table (2).

8.1. Numerical verification of equilibrium points. This section initially involves the computation and numerical verification of the parametric conditions pertaining to the existence and stability of the equilibrium points. The values of the parameters utilised in figure (3) are as follows: $r_1 = 0.5$, $r_2 = 0.5$, $r_3 = 0.5$, $r_4 = 0.5$, $r_5 = 0.5$, $b = 1$, $\gamma = 0.5$, $d_1 = 1$, and $d_2 = 1$. The analysis of the figure (3) reveals that the proposed system (2) exhibits local asymptotic stability in the vicinity of the axial equilibrium point $E_1(1,0,0)$. In addition, we numerically compute the Jacobian matrix at the axial equilibrium point $E_1(1,0,0)$. The eigenvalues of the Jacobian matrix at $E_1(1,0,0)$ are -1, -0.5, and -0.625. Given that all of the eigenvalues are negative, it can be inferred that the axial equilibrium point $E_1(1,0,0)$ exhibits local asymptotic stability.

The set of parametric values, namely $r_1 = 0.215606$, $r_2 = 0.901961$, $r_3 = 0.852217$, $r_4 = 0.927631$, $r_5 = 0.043929$, $b = 0.267475$, $\gamma = 1$, $d_1 = 0.852217$, and $d_2 = 0.826533$, were utilised

Parameter	values
r_1	0.875
r_2	0.031
r_3	19.518
r_4	1
r_5	1.5
b	0.8
γ	2
d_1	1
d_2	1

TABLE 2. *The values assigned to the parameters that are associated with system (2).*

to generate the phase portrait depicted in figure (4). The figure (4) indicates that the solutions converge towards the boundary equilibrium point (0.665631, 0.0479866, 0). Following some computations, the values of K_1, K_2, and K_3 (as specified in theorem (1)) are determined through numerical methods for the abovementioned set of parameters. It is found that $K_1 = 1.958 > 0$, $K_2 = 2.66385 > 0$, $K_3 = 1.50779 > 0$, and $K_1K_2 - K_3 = 3.70803 > 0$. Therefore, based on the Routh-Hurwitz criteria, it can be concluded that the boundary equilibrium point denoted as E_2 exhibits asymptotic stability given the specified parametric conditions. The Jacobian matrix is computed at the equilibrium point E_2, and its corresponding eigenvalues are -0.824603, $-0.0861618 + 0.280297i$, and$-0.0861618 - 0.280297i$. The negative real parts of all eigenvalues serve as evidence for the asymptotic stability of E_2 under the given parametric conditions. In order to establish the asymptotic stability of the interior equilibrium point $E^{'}$, the parameter values presented in the table (2) are taken into consideration. Also, figure (5a) has been generated utilising the same parametric values given in the table (2). The figure (5a) depicts that the solutions tend to converge towards the interior equilibrium point $E^{'}(0.861111, 1.42857, 0.92166)$. Upon conducting computational analysis, the numerical values of L_1, L_2, and L_3 (as stated in theorem (1)) were ascertained for the aforementioned set of

parametric values. The results indicate that $L_1 = 0.600966$, $L_2 = 0.293992$, $L_3 = 0.166667$, and $L_1L_2 - L_3 = 0.0100125$, all of which are greater than zero. The conclusion can be drawn that the interior equilibrium point $E^{'}$ demonstrates the local asymptotic stability under the given parametric conditions, as per the Routh-Hurwitz criteria. Furthermore, the Jacobian matrix is evaluated at the equilibrium point $E^{'}$. The resulting eigenvalues associated with this Jacobian matrix are -0.585235 , $-0.00786537 + 0.533596i$, $-0.00786537 - 0.533596i$. The presence of negative real parts in all eigenvalues provides substantiation for the local asymptotic stability of $E^{'}(0.861111, 1.42857, 0.92166)$ given the specified parametric conditions.

As depicted in figure (3b), the solution trajectories of system (2) exhibit convergence towards the axial equilibrium point E_1, although starting from four different coexistent initial values. This observation indicates the global stability of the axial equilibrium point. Furthermore, in a comparable manner, the diagram depicted in figure (5b) illustrates the global stability of the interior equilibrium point E^i, as numerous coexisting initial values tend to converge towards it.

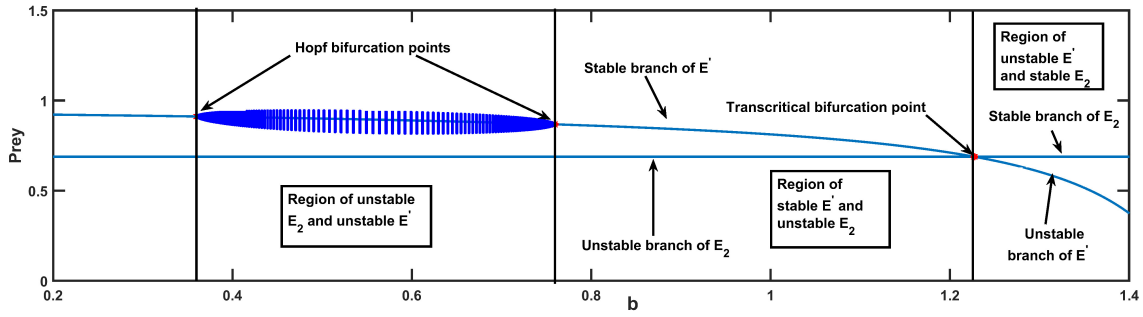

FIGURE 6. *The presence of Hopf bifurcations and transcritical bifurcation within the equilibrium curve of the interior equilibrium is illustrated.*

8.2. The impact of the parameter b on population stability. This section explores the impact of the constant b on model (2), while holding the remaining parameters constant as specified in the table, and manipulating the value of the constant b. The aforementioned figure (see figure (6)) is generated through the exclusive manipulation of the parameter b within the predetermined set of parameters outlined in table (2). The figure (6) illustrates that at two distinct values of the parameter b, specifically at $b = 0.359982 = b^{H_1}$ and $b = 0.759499 = b^{H_2}$, two

Hopf bifurcation takes place. Initially, when $b = 0$, all three species coexist within the ecosystem due to the stability of the interior equilibrium point (see figure (7a)). The numerical values obtained for L_1, L_2, and L_3 are $0.854167 > 0$, $0.788254 > 0$, and $0.536355 > 0$, respectively. The value of $L_1L_2 - L_3$, which is 0.136945, is also greater than zero. These results indicate that the local stability of $E^{'}$ is established. As the parameter b is incremented, the stability of the interior equilibrium experiences a transition and becomes unstable due to the emergence of a Hopf bifurcation at $b = 0.359982 = b^{H_1}$, resulting in the appearance of periodic solutions (see figures (7c) and (8b)). Upon reaching a certain threshold, specifically at $b = 0.759499 = b^{H_2}$, another Hopf bifurcation occurs resulting in the stabilisation of the coexisting equilibrium point (see figures (7e) and (8d)). Upon increasing the value of parameter b substantially, an alteration in the stability of the interior equilibrium point is detected, resulting in its instability due to a transcritical bifurcation occurring at $b = 1.227086 = b^{tb}$. Consequently, the top predator free equilibrium point E_2 attains stability . This can be confirmed by selecting a parameter value for b that exceeds b^{tb}. Upon setting $b = 1.6$, the values of K_i for $i = 1,2,3$ are determined. The computed values are as follows: $K_1 = 2.31385 > 0$, $K_2 = 5.33206 > 0$, $K_3 = 0.256531 > 0$, and $K_1K_2 - K_3 = 12.0811 > 0$. Consequently, applying the Routh-Hurwitz criteria, it can be inferred that the equilibrium point E_2, which is devoid of top predators, is locally stable .

Additionally, we quantitatively verify Hopf bifurcations' presence, directional change, and stability. It is found that $L_1(b^{H_1}) = 0.71 > 0$, $L_2(b^{H_1}) = 0.51 > 0$, $L_3(b^{H_1}) = 0.36 > 0$, $L_1(b^{H_1})L_2(b^{H_1}) - L_3(b^{H_1}) = 0$, and $L_1(b^{H_1})L_2'(b^{H_1}) + L_2(b^{H_1})L_1'(b^{H_1}) - L_3'(b^{H_1}) = -0.199052 \neq 0$. which further supports the fact that a Hopf bifurcation occurs at $b = 0.359982 = b^{H_1}$. In other words, it meets the NASC (as stated in Theorem (5)) required for Hopf bifurcation to exist. Now, we use the procedures described by Hazzard [37] to determine the nature and direction of bifurcating periodic solutions for the parameter values given in table (2) with $b = b^{H_1}$, and we find $C_1(0) = -2.44877 - 17.8463i$, $\mu_2 = -51.1664 < 0$, $\beta_2 = -4.89754 < 0$, and $\alpha^{'}(0) = -0.0478589 < 0$. The Hopf bifurcation that takes place at $b = b^{H_1}$ is characterised by its supercritical nature, as evidenced by the negative values of μ_2 and $\alpha^{'}(0)$ in tandem with the negative value of β_2, as stated in theorem (6). In addition, the value of first Lyapunov coefficient is $-2.808933e^{-2} < 0$.

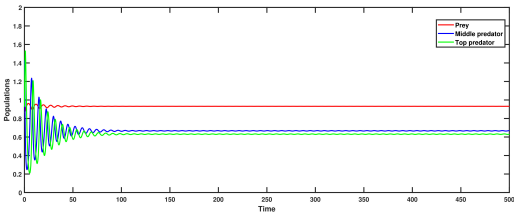

(A) *Time series at $b = 0$ and the rest parameter values are from table (2)*

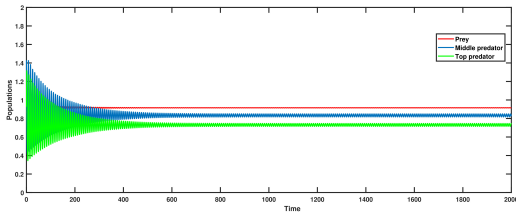

(B) *Time series at $b = 0.3$ and the rest parameter values are from table (2)*

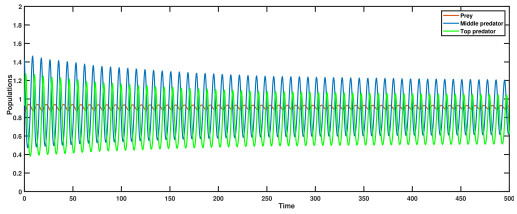

(C) *Time series at $b = 0.359982$ and the rest parameter values are from table (2)*

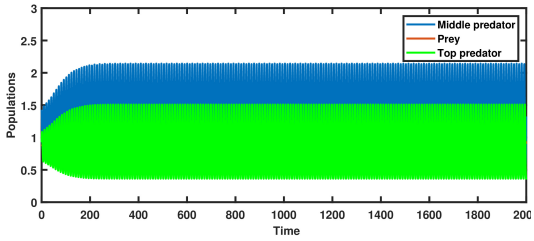

(D) *Time series at $b = 0.6$ and the rest parameter values are from table (2)*

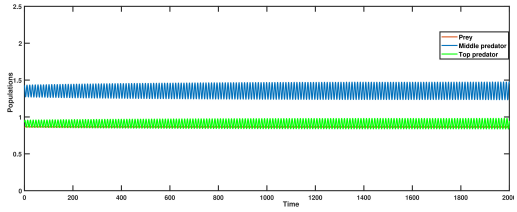

(E) *Time series at $b = 0.759499$ and the rest parameter values are from table (2)*

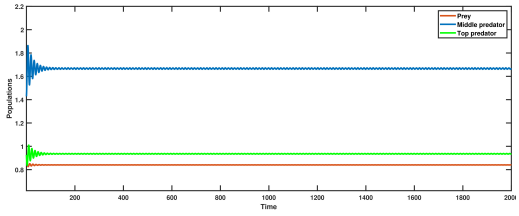

(F) *Time series at $b = 0.9$ and the rest parameter values are from table (2)*

FIGURE 7. *Time series showing alteration in population dynamics at various values of the parameter b taking initial population (0.86,1.42,0.92).*

In a similar way, we compute $L_1(b^{H_2}) = 0.605 > 0$, $L_2(b^{H_2}) = 0.305 > 0$, $L_3(b^{H_2}) = 0.184 > 0$, $L_1(b^{H_2})L_2(b^{H_2}) - L_3(b^{H_2}) = 0$, and $L_1(b^{H_2})L_2'(b^{H_2}) + L_2(b^{H_2})L_1'(b^{H_2}) - L_3'(b^{H_2}) = 0.209134 \neq 0$. This finding provides additional evidence that a Hopf bifurcation transpires at $b = 0.759499 = b^{H_2}$ as neccesary and sufficient condition for the manifestation of Hopf bifurcation is satisfied for the parameter values explicated in table (2) with $b = b^{H_2}$ (refer to theorem (5)). Additionally, it is observed that $C_1(0) = -3.9825 - 6.54994i$, $\mu_2 = -21.0693 < 0$, $\beta_2 = -7.96501 < 0$, and $\alpha'(0) = -0.189019 < 0$. The occurrence of the Hopf bifurcation at

$b = b^{H_1}$ is identified as being of a supercritical nature, as indicated by the concomitant positive value of μ_2 $\alpha^{'}(0)$ and negative value of β_2, in accordance with theorem (6). Furthermore, it is noteworthy that the first Lyapunov coefficient holds a value of $-6.426589e^{-2}$, indicating a negative value.

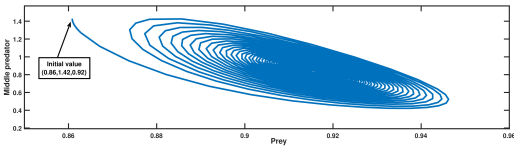

(A) *Prey vs Middle predator phase portrait at* $b = 0.3$ *with the remainder of the parameters taken from the table (2)*

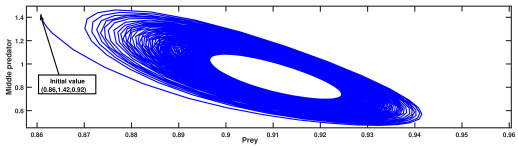

(B) *Prey vs Middle predator phase portrait at* $b = 0.359982$ *with the remainder of the parameters taken from the table (2)*

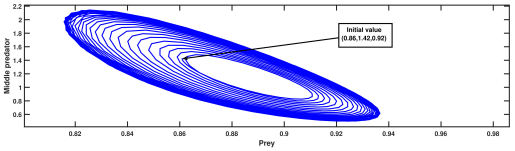

(C) *Prey vs Middle predator phase portrait at* $b = 0.6$ *with the remainder of the parameters taken from the table (2)*

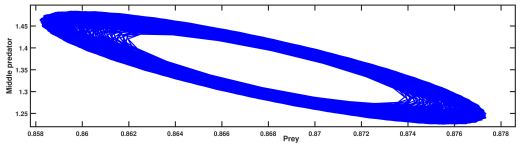

(D) *Prey vs Middle predator phase portrait at* $b = 0.759499$ *with the remainder of the parameters taken from the table (2)*

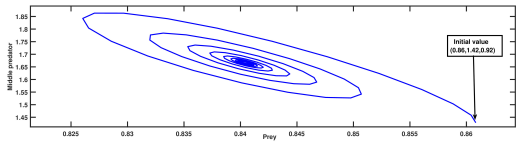

(E) *Prey vs Middle predator phase portrait at* $b = 0.9$ *with the remainder of the parameters taken from the table (2)*

FIGURE 8. *The two-dimensional phase portraits serve as visual representations of the changes in parameters and their corresponding impacts on the populations of the prey, middle predator, and top predator.*

8.3. Influence of prey odour on population dynamics. The objective of this section is to examine the behaviour of the system (2) when prey odour is present. In order to conduct our investigation, we utilised parameter values identical to those presented in table (2), with the exception of the parameter γ which denotes the impact of odour. The figure depicted in figure

(9) is generated using identical parameter values as those previously stated, with the exception of the parameter γ, which is varied.

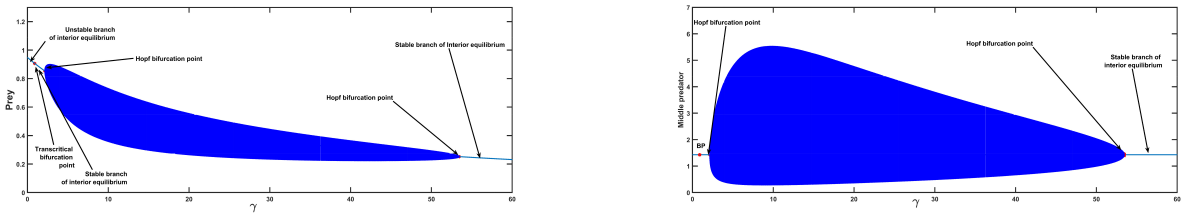

(A) *Prey vs* γ (B) *Middle predator vs* γ

FIGURE 9. *Bifurcation diagrams in relation to the parameter* γ.

The analysis of figure (9) suggests the occurrence of two distinct Hopf bifurcations at different parameter values of γ. At the initial setting of $\gamma = 0$, the axial equilibrium point is deemed stable (see figure (10a)). This is due to the negative eigenvalues of the Jacobian matrix $J_{(1,0,0)}$, which are -1, -0.875, and -0.389921. These eigenvalues satisfy the Routh-Hurwitz criteria for stability. On the contrary, it should be noted that the interior equilibrium point exhibits instability, given that $L_3 = -0.163156 < 0$. As the parameter γ increases, a transcritical bifurcation occurs at $\gamma = 0.635785 = \gamma^{tb_1}$, resulting in a swap of stability between the equilibrium points E_1 and E_2 (see figures (10a) and (10b)). Consequently, the stability of boundary equilibrium point E_2 is established while the instability of axial equilibrium E_1 is confirmed through the examination of the eigenvalues of the Jacobian matrices $J_{(1,0,0)}$ and $J_{(A_1,B_1,0)}$ at some $\gamma = 0.64 > \gamma^{tb_1}$ (see figure 10b) . Specifically, the eigenvalues of $J_{(1,0,0)}$ are $-1 < 0$, $-0.875 < 0$, and $0.000529644 > 0$, while the eigenvalues of $J_{(A_1,B_1,0)}$ are $-0.990297 < 0$, $-0.874267 < 0$, and $-0.00052983 < 0$. Upon a subsequent increase in the parameter γ, a transcritical bifurcation arises at $\gamma = 0.883166 = \gamma^{tb_2}$, resulting in the stabilisation of the interior equilibrium $E^{'}$ and the destabilisation of the boundary equilibrium point E_2 (see figure (10c)). This can be confirmed via examining the eigenvalues of $J_{(A_1,B_1,0)}$ at some value $\gamma = 0.9 > \gamma^{tb_2}$, which are $-0.634244 < 0$, $-0.302155 < 0$, and $0.0178547 > 0$. The computed values, namely $L_1 = 0.8274 > 0$, $L_2 = 0.118336 > 0$, $L_3 = 0.00214824 > 0$, and $L_1L_2 - L_3 = 0.095763$ at $\gamma = 0.9 > \gamma^{tb_2}$, provide evidence for the stability of the interior equilibrium. By increasing the

parameter γ beyond a certain threshold value, specifically $\gamma = 2.114911 = \gamma^{H_1}$, a Hopf bifurcation occurs, resulting in the emergence of periodic solutions and rendering the interior equilibrium point unstable (see figures (10d) and (11b)). However, at a higher value of γ, specifically $\gamma = 54.624314 = \gamma^{H_2}$, another Hopf bifurcation occurs, which actually stabilises the interior equilibrium point (see figures (10f) and (11d)). The existence of the aforementioned Hopf bifurcations is numerically validated through the utilisation of theorem (5). We find, the values $L_1(\gamma^{H_1}) = 0.58011 > 0$, $L_2(\gamma^{H_1}) = 0.314398 > 0$, $L_3(\gamma^{H_1}) = 0.18182 > 0$, , $L_1(\gamma^{H_1})L_2(\gamma^{H_1}) - L_3(\gamma^{H_1}) = 0$, and $L_1(\gamma^{H_1})L_2'(\gamma^{H_1}) + L_2(\gamma^{H_1})L_1'(\gamma^{H_1}) - L_3'(\gamma^{H_1}) = -0.0829853 \neq 0$ and hence, the verification of the existence of Hopf bifurcation at $\gamma = 2.114911 = \gamma^{H_1}$ has been established in accordance with theorem (5). In a similar vein, it is observed that $L_1(\gamma^{H_2}) = 0.166051 > 0$, $L_2(\gamma^{H_2}) = 2.8744 > 0$, and $L_3(\gamma^{H_2}) = 0.48266 > 0$, $L_1(\gamma^{H_2})L_2(\gamma^{H_2}) - L_3(\gamma^{H_2}) = 0$, and $L_1(\gamma^{H_2})L_2'(\gamma^{H_2}) + L_2(\gamma^{H_2})L_1'(\gamma^{H_2}) - L_3'(\gamma^{H_2}) = 0.0365616 \neq 0$ serves as evidence for the occurrence of Hopf bifurcation at $\gamma = 54.624314 = \gamma^{H_2}$, as stipulated by theorem (5).

Now, the methodology outlined by Hazzard [37] is employed to ascertain the characteristics and direction of bifurcating periodic solutions for the parameter values specified in table (2) when $\gamma = 2.114911 = \gamma^{H_1}$. After some calculations, it is found that $C_1(0) = -4.14409 - 5.71554i$, $\mu_2 = 22.332 > 0$, $\beta_2 = -8.28818 < 0$, and $\alpha^{'}(0) = 0.185567 > 0$. In accordance with the theorem (6), the negative values of μ_2 and $\alpha^{'}(0)$ in combination with the negative value of β_2, establish the Hopf bifurcation's supercritical nature at $\gamma = 2.114911 = \gamma^{H_1}$. Additionally, the primary Lyapunov coefficient associated with this Hopf bifurcation is calculated to be $-6.939086e^{-2}$. In a similar manner, using the parameter values specified in table (2), with the exception of γ, which is set to $\gamma^{H_2} = 54.624314$, we obtain $C_1(0) = -23.5456 - 40.7732i$, $\mu_2 = 2730.21 > 0$, $\beta_2 = -47.0912 < 0$, and $\alpha^{'}(0) = 0.00862411 > 0$. As per theorem (6), the Hopf bifurcation under consideration exhibits a supercritical characteristic. Furthermore, the first Lyapunov coefficient pertaining to the aforementioned Hopf bifurcation is calculated to be $-2.759372e^{-1}$.

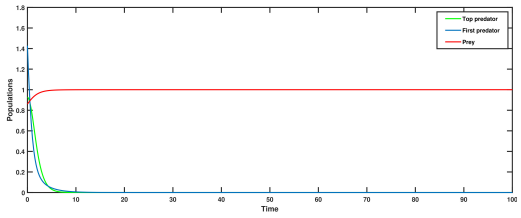

(A) *Time series with $\gamma = 0$, and the rest of the parameter values are taken from (2) with initial value (0.86,1.42,0.92)*

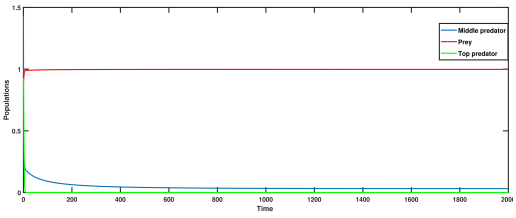

(B) *Time series with $\gamma = 0.64$, and the rest of the parameter values are taken from (2) with initial value (0.86,1.42,0.92)*

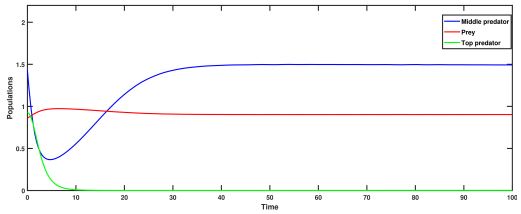

(C) *Time series with $\gamma = 0.9$, and the rest of the parameter values are taken from (2) with initial value (0.86,1.42,0.92)*

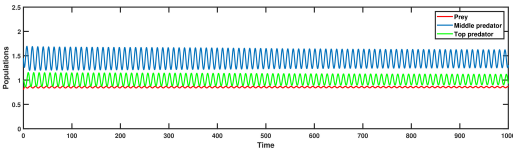

(D) *Time series with $\gamma = 2.11491$, and the rest of the parameter values are taken from (2) with initial value (0.8,1.45,1)*

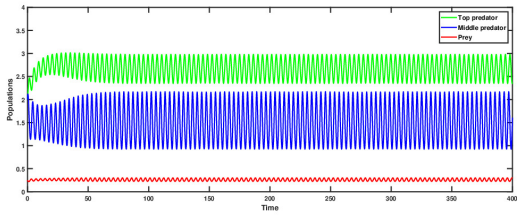

(E) *Time series with $\gamma = 50$, and the rest of the parameter values are taken from (2) with initial value (0.25,2,2).*

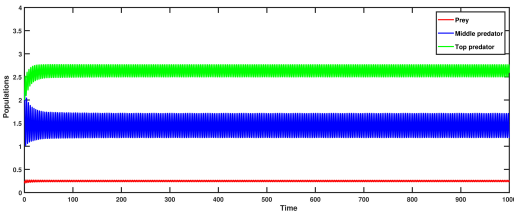

(F) *Time series with $\gamma = 54.62431$, and the rest of the parameter values are taken from (2) with initial value (0.25,2,2)*

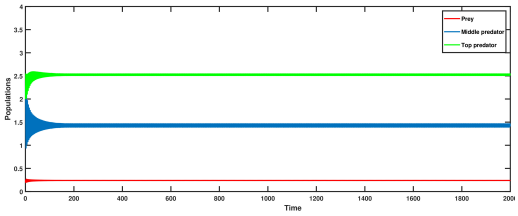

(G) *Time series with $\gamma = 58$, and the rest of the parameter values are taken from (2) with initial value (0.25,2,2)*

FIGURE 10. *Time series showing how the dynamics of a population change at different values of the parameter γ.*

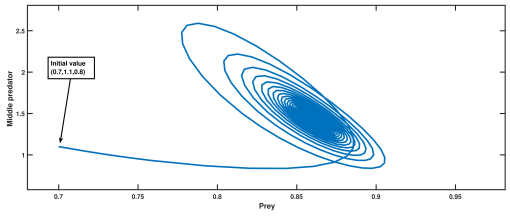

(A) *Prey vs Middle predator with* $\gamma = 2$ *and the remaining parameter values from the table (2)*

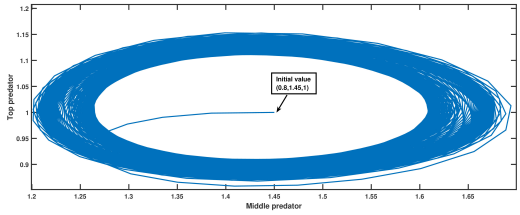

(B) *Middle predator vs Top predator with* $\gamma = 2.11$ *and the rest parameter values from the table (2)*

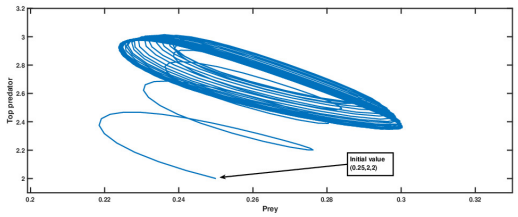

(C) *Prey vs Middle predator with* $\gamma = 50$ *and the rest parameter values from the table (2)*

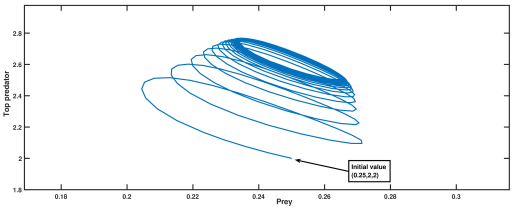

(D) *Prey vs Top predator with* $\gamma = 54.62431$ *and the rest parameter values from the table (2)*

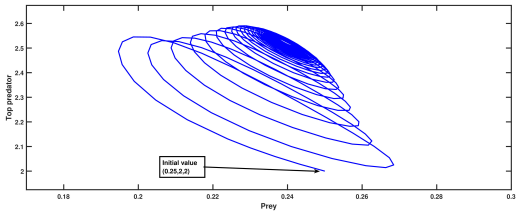

(E) *Prey vs Top predator with* $\gamma = 58$ *and the rest parameter values from the table (2)*

FIGURE 11. *Phase portraits depicting alterations in the parameter and their impact on the populations of top predator, middle predator, and prey in a two-dimensional space.*

8.4. Impact of the intake rate parameter r_2 on the system. The parameter r_2 in the biosystem (2) is positively correlated with the consumption rate of middle predators on prey. To assess the impact of the parameter r_2, we employ parameter values as outlined in table (2). By varying

the parameter value of r_2 while keeping the other parameters consistent with those presented in table (2), we have generated figure (12).

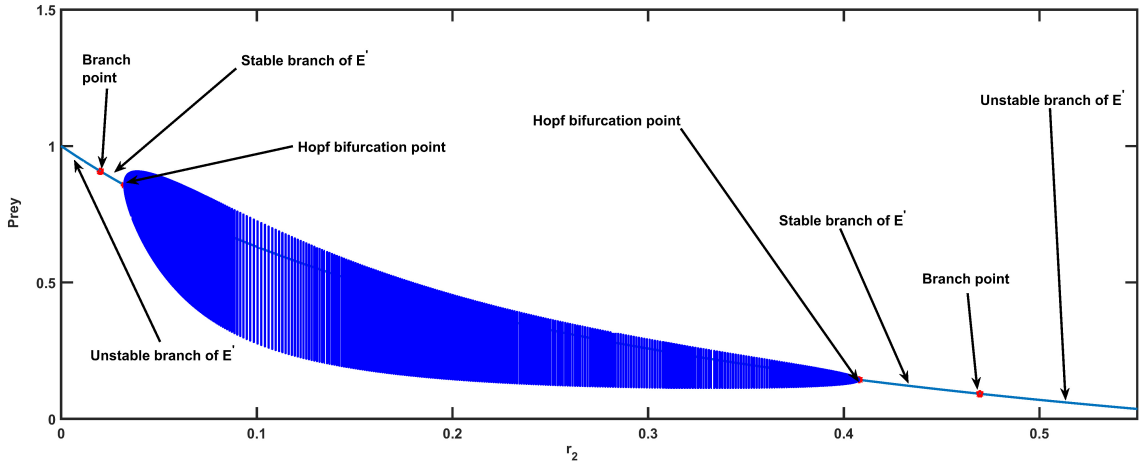

FIGURE 12. *The bifurcation diagram exhibits the presence of Hopf bifurcations and transcritical bifurcations across distinct values of the parameter* r_2.

The occurrence of a Hopf bifurcation is apparent at the parameter value $r_2 = 0.032321 = r_2^{H_1}$, as depicted in figure (12). In terms of numerical values, it can be observed that $L_1(r_2^{H_1}) = 0.579743 > 0, L_2(r_2^{H_1}) = 0.31138 > 0, L_3(r_2^{H_1}) = 0.180643 > 0, , L_1(r_2^{H_1})L_2(r_2^{H_1}) - L_3(r_2^{H_1}) = 0.$ and $L_1(r_2^{H_1})L_2'(r_2^{H_1}) + L_2(r_2^{H_1})L_1'(r_2^{H_1}) - L_3'(r_2^{H_1}) = -9.5425 \neq 0$ which verifies the existence of Hopf bifurcation at $r_2 = 0.032321 = r_2^{H_1}$. The Hopf bifurcation results in the destabilisation of the interior equilibrium point (see figures (13b) and (14b)). The confirmation of the Hopf bifurcation's supercritical nature can be established through the following conditions: $C_1(0) = -4.10878 - 5.6722i$, $\mu_2 = 0.208626 > 0$, $\beta_2 = -8.21757 < 0$, and $\alpha'(0) = 19.6945 > 0$. By sufficiently reducing the parameter r_2, the stability of the interior equilibrium point is lost as a result of a transcritical bifurcation that takes place at $r_2 = 0.020042 = r_2^{tb_1}$. Consequently, the boundary equilibrium point attains stability. Subsequent to further reduction in the parameter r_2, an additional transcritical bifurcation arises at $r_2 = 0.017078 = r_2^{tb_2}$. As a result of this bifurcation, the boundary equilibrium point undergoes a loss of stability to the axial equilibrium point and becomes unstable.

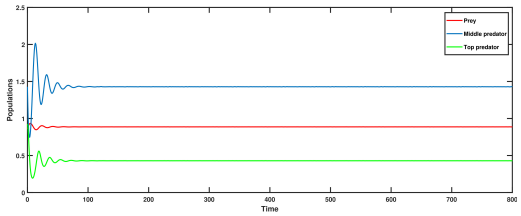

(A) *The time series of all three populations at* $r_2 = 0.025$*, along with the remaining parameter values listed in table (2).*

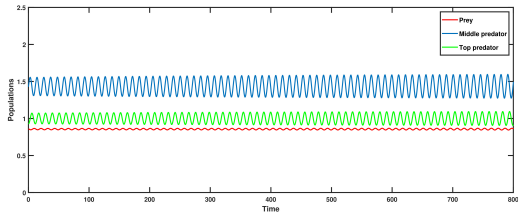

(B) *The time series of all three populations at* $r_2 = 0.032321$*, along with the remaining parameter values listed in table (2).*

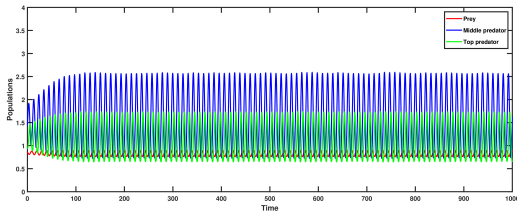

(C) *Time series of all three populations with* $r_2 = 0.035$ *and the remaining parameter values from the table (2).*

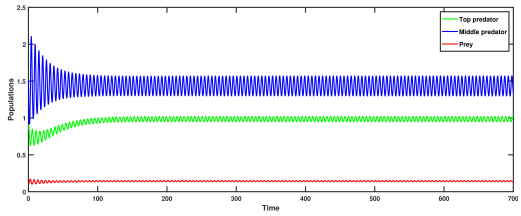

(D) *Time series of all three populations with* $r_2 = 0.407799$ *and the remaining parameter values from the table (2).*

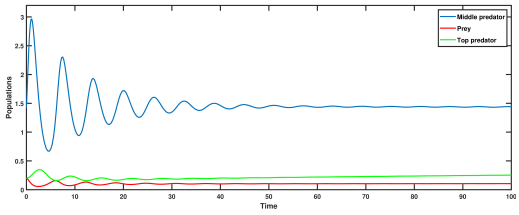

(E) *Time series of all three populations at* $r_2 = 0.45$ *and rest parameter values from the table (2).*

FIGURE 13. *The temporal progression of the prey, middle predator, and top predator populations is depicted, highlighting distinct trends in their population dynamics over time at different values of the parameter* r_2*.*

Added to that, it appears that another supercritical Hopf bifurcation emerges at the specific parameter value of $r_2 = 0.407799 = r_2^{H_2}$, as depicted in figures (12), (13d), and (14d), which results in the stabilisation of the interior equilibrium point (see figures (13e) and (14e)).

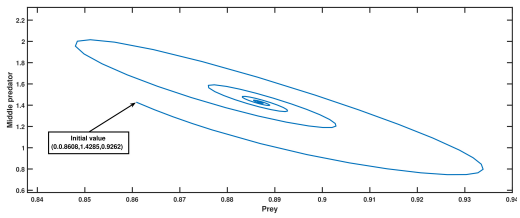

(A) *Prey vs Middle predator at* $r_2 = 0.025$ *with the rest parameter values from the table (2)*

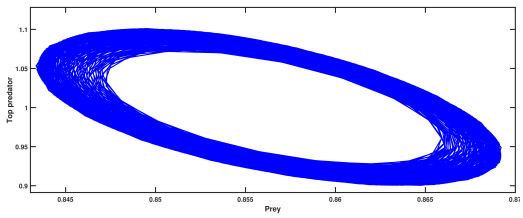

(B) *Prey vs Top predator at* $r_2 = 0.032321$ *with the rest parameter values from the table (2)*

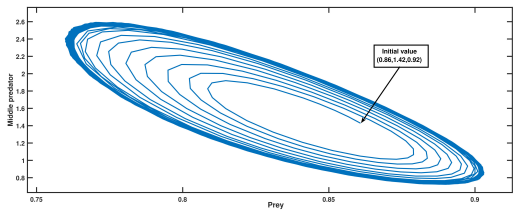

(C) *Prey vs Middle predator at* $r_2 = 0.035$ *with the rest parameter values from the table (2)*

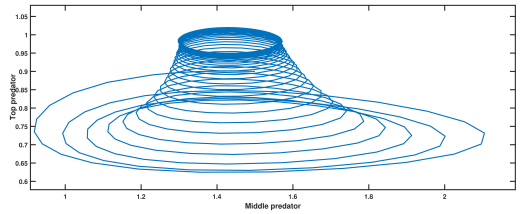

(D) *Middle predator vs Top predator at* $r_2 = 0.407799$ *with rest parameter values from table (2)*

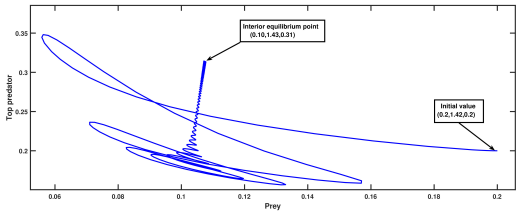

(E) *Prey vs Top predator at* $r_2 = 0.45$ *with the rest parameter values from the table (2)*

FIGURE 14. *Phase portraits in a two-dimensional space are depicted which illustrate the impact of parameter variations on the dynamics of populations.*

The existence of the aforementioned Hopf bifurcation can be established numerically. In this context, we calculate, $L_1(r_2^{H_1}) = 0.0426723 > 0$, $L_2(r_2^{H_1}) = 1.49132 > 0$, $L_3(r_2^{H_1}) = 0.0639071 > 0$, , $L_1(r_2^{H_1})L_2(r_2^{H_1}) - L_3(r_2^{H_1}) = 0$, and $L_1(r_2^{H_1})L_2'(r_2^{H_1}) + L_2(r_2^{H_1})L_1'(r_2^{H_1}) - L_3'(r_2^{H_1}) = 4.9649 \neq 0$ and its verification is established by theorem (5). In order to confirm the type of Hopf bifurcation under consideration, the following conditions were evaluated: $C_1(0) = -36.5099 - 86.5669i$, $\mu_2 = 47.5052 > 0$, $\beta_2 = -73.0199 < 0$, and $\alpha'(0) = 0.768546 > 0$.

These conditions establish the supercritical nature of the Hopf bifurcation being discussed, in line with theorem (6). At the critical value of the parameter $r_2 = 0.469544 = r_2^{tb_3}$, an additional transcritical bifurcation arises, resulting in the instability of the interior equilibrium and the stability of the boundary equilibrium point.

8.5. Effects of growth rate of prey r_1 and death rates of the two predator species d_1 and d_2 on the food chain. The intrinsic growth rate of prey denotes the theoretical maximum rate at which a population of prey can expand in optimal circumstances, without any constraining factors such as resource scarcity, competition, or predation. The parameter r_1 in the biosystem (2) is associated with the intrinsic growth rate of the prey. By keeping all parameter values constant as specified in table (2), with the exception of r_1, and manipulating r_1 as a variable, we have generated figure (15a). A transcritical bifurcation occurs when the parameter value r_1 reaches its critical value of $r_1^{tb} = 0.341143$. Consequently, the stability of the interior equilibrium is achieved, although the occurrence of a supercritical Hopf bifurcation at the critical value of $r_1 = 0.923231 = r_1^H$, destabilises the interior equilibrium point. This observation is readily discernible from figure (15a).

The mortality rate is a crucial ecological metric that impacts various aspects of population dynamics, species relationships, community organisation, ecosystem operation, and conservation endeavours. The variables d_1 and d_2 represent the mortality rates of the middle predator and top predator, respectively, within the biosystem (2). The graphical representation depicted in figure (15b) was constructed utilising the parameter values explicated in table (2), while solely manipulating the parameter d_1. Similarly, figure (15c) has been generated utilising the parameter values explicated in table (2), while solely altering the parameter d_2. The occurrence of a backward bifurcation is depicted in figure (15b) at the critical value of the parameter $d_1 = 0.982152 = d_1^H$, which results in the stabilisation of the interior equilibrium. However, a transcritical bifurcation transpires at $d_1 = 1.432262 = d_1^{tb}$, rendering the previously stable equilibrium unstable. A comparable situation is illustrated in figure (15c). The presence of a backward Hopf bifurcation is detected at $d_2 = 0.978465 = d_2^H$, as depicted in figure (15c), resulting in the stabilisation of the interior equilibrium. Moreover, a transcritical bifurcation

occurs at $d_2 = 1.398062 = d_2^{tb}$, resulting in a shift in the stability of the interior equilibrium point.

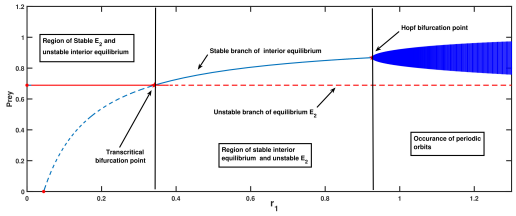

(A) *Bifurcation diagram with respect to the parameter r_1*

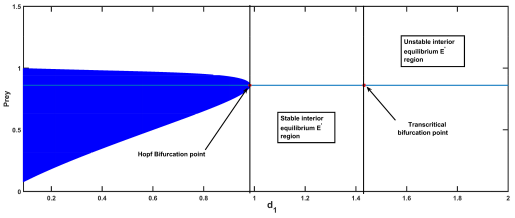

(B) *Bifurcation diagram with respect to the parameter d_1*

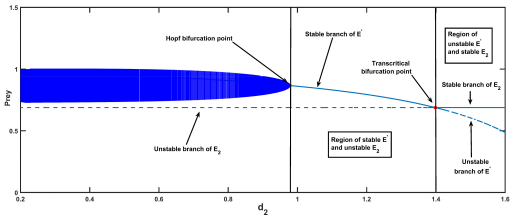

(C) *Bifurcation diagram with respect to the parameter d_2*

FIGURE 15. *The bifurcation diagrams with respect to various parameters are provided, illustrating the existence of various bifurcations.*

9. SUMMARY

The biological process of predator-prey relationship is a fundamental subject in the field of ecology. It is very much evident that prey and predators utilise various strategies to maximise their biomass and increase their chances of survival. One such strategy employed by predators is to utilise the olfactory cues of their prey in order to enhance their likelihood of successful predation. The objective of this manuscript is to investigate a mathematical framework that represents a food chain system involving prey (s), intermediate predator, i.e, middle predator (p_1), and apex predator, i.e, top predator (p_2). The consistent utilisation of prey odour is assumed to aid the middle predator population in predation. The inclusion of prey odour into this predator-prey population model enhances its realism. The model assumes that the middle predator exhibits a linear functional response in consuming its prey, while top predator also

utilise a Holling type II functional response in hunting its own prey i.e, middle predator. The dynamics of model (2) have been subjected to theoretical analysis to derive insights pertaining to its long-term behaviour. Theoretical evidences have been provided regarding the positiveness and boundedness of the solutions of the system (2). Subsequently, various equilibrium points were identified and subjected to a local stability analysis. The global stability of both the axial equilibrium point and the interior equilibrium point has been examined. A comprehensive numerical analysis has been performed to examine the Hopf bifurcation phenomenon with respect to several parameters. These parameters include the intake rate of middle predators (r_2), the intrinsic growth rate of prey (r_1), the coefficient of odour effect (γ), and the death rates of both predator species (d_1 and d_2), as well as the handling time of middle predators (the top predator's prey) by the top predator during predation (b). The findings are thoroughly addressed, providing insights into the impact of odour effect on the interactions within the food chain system. Additionally, we conducted a numerical investigation into the effects of the remaining parameters and illustrated our findings through the use of figures, which offer enhanced visual representation and ease of comprehension for a broader audience. The findings indicate that the dynamics of this system can be highly diverse, contingent upon the parameter ranges. These dynamics encompass the attainment of a solitary co-existence equilibrium, the eradication of either the top predator or both predator populations, and the persistence of oscillations or periodic behaviour. Upon examination of the model, it has been determined that the trivial equilibrium point functions as a saddle point, thereby precluding the possibility of the extinction of all three species. Additionally, it has been observed that the axial equilibrium, boundary equilibrium, and interior equilibrium states exhibit asymptotic stability under certain parametric constraints, as depicted in figures (3a), (4), and (5a). Moreover, the presence of the top predator free equilibrium negates the stability of the equilibrium solely occupied by the prey. Under certain parametric conditions, the prey-only equilibrium and the interior equilibrium can attain global stability, as demonstrated in figures (3b) and (5b) respectively.

Our numerical investigation into the influence of the odor-related parameter has yielded noteworthy and significant findings, demonstrating the manner in which the odour effect impacts long-term population dynamics. The absence of the odour effect in the model (2) has been

observed to render the coexistence of all three species unattainable, ultimately leading to the collapse of the food chain (refer to figures (9) and (10a)). As the level of odour influence intensifies, the middle predator's viability is established through a transcritical bifurcation, and with subsequent elevations, the sustainability of all three species is affirmed via an additional transcritical bifurcation. At a certain threshold of odour impact, a Hopf bifurcation occurs in the population dynamics of system (2), resulting in periodic oscillation. The system is subsequently stabilised at a specific parameter value through another Hopf bifurcation (refer to figures (9), (10), and (11)).

The handling time of middle predators by the top predator during predation has been noted to play a significant role in the biosystem (2). The coexistence of all three species can be achieved when handling time is negligible, as depicted in figures (6) and (7a). Additionally, periodic fluctuations in the population of the three species arise from two supercritical Hopf bifurcations that take place at distinct values of the parameter linked to handling time. Furthermore, it has been observed that a transcritical bifurcation transpires at a specific value of the parameter b, which results in an alteration of the stability of the coexistence equilibrium state (refer to figures (6), (7), and (8)).

Analogously, the system (2) exhibits intriguing dynamics with respect to the intake rate (r_2), prey growth rate (r_1), and the death rates of both predators (d_1 and d_2). As the intake rate r_2 varies, periodic fluctuations in the population dynamics of the system (2) are observed due to the existence of two supercritical Hopf bifurcations. Also, two transcritical bifurcations occur at different intake rates, indicating that it plays a significant role in sustaining all three species in the food chain (refer to figures (12), (13), and (14)). The population stability within the system (2) is also influenced by the intrinsic growth rate of the prey (r_1). At a specific value of the growth rate parameter of prey r_1, a Hopf bifurcation is observed in the biosystem, leading to the emergence of periodic oscillations. Additionally, the intrinsic growth rate of the prey causes a transcritical bifurcation to occur (see figure (15a)).The population dynamics in the biosystem (2) are impacted by the mortality rates of both predators, denoted as d_1 and d_2 respectively. Periodic variations resulting from Hopf bifurcations and changes in the stability of the interior

equilibrium due to transcritical bifurcations can be detected across various values of the parameters related to the death rates of the two predator species, namely d_1 and d_2 (see figure (15)). This research provides evidence to substantiate the perspective that the odour of prey can serve as a pivotal element in maintaining cohabitation within a model comprising of multiple species. In future research, it would be of academic interest to broaden the realism of the system (2) by incorporating real-world authentic data to estimate the parameters.

FUNDING

This work is supported by Council of Scientific and Industrial Research(CSIR), Ministry of Science & Technology, Govt. of India (File no: 09/0059(15235)/2022-EMR-I).

CONFLICT OF INTERESTS

The authors declare that there is no conflict of interests.

REFERENCES

[1] A.J. Lotka, Elements of physical biology, Williams and Wilkins, Baltimore, (1925).

[2] V. Volterra, Variazioni e fluttuazioni del numero d'individui in specie animali conviventi, Memoria della Reale Accademia Nazionale dei Lincei, 2 (1926), 31-113.

[3] P.A. Braza, Predator–prey dynamics with square root functional responses, Nonlinear Anal.: Real World Appl. 13 (2012), 1837-1843. https://doi.org/10.1016/j.nonrwa.2011.12.014.

[4] B. Barman, B. Ghosh, Role of time delay and harvesting in some predator-prey communities with different functional responses and intra-species competition, Int. J. Model. Simul. 42 (2021), 883-901. https://doi.org/10.1080/02286203.2021.1983747.

[5] X. Jiao, X. Li, Y. Yang, Dynamics and bifurcations of a Filippov Leslie-Gower predator-prey model with group defense and time delay, Chaos Solitons Fractals. 162 (2022), 112436. https://doi.org/10.1016/j.chaos.2022.112436.

[6] M. Peng, R. Lin, Y. Chen, et al. Qualitative analysis in a Beddington-DeAngelis type predator-prey model with two time delays, Symmetry. 14 (2022), 2535. https://doi.org/10.3390/sym14122535.

[7] J. Li, X. Liu, C. Wei, The impact of role reversal on the dynamics of predator-prey model with stage structure, Appl. Math. Model. 104 (2022), 339-357. https://doi.org/10.1016/j.apm.2021.11.029.

[8] P. Panja, Dynamics of a stage structured predator-prey model with fear effects, Discontin. Nonlinear. Complex. 11 (2022), 651-669. https://doi.org/10.5890/dnc.2022.12.007.

[9] S. Pal, N. Pal, S. Samanta, J. Chattopadhyay, Effect of hunting cooperation and fear in a predator-prey model, Ecol. Complex. 39 (2019), 100770. https://doi.org/10.1016/j.ecocom.2019.100770.

[10] N.C. Pati, G.C. Layek, N. Pal, Bifurcations and organized structures in a predator-prey model with hunting cooperation, Chaos Solitons Fractals. 140 (2020), 110184. https://doi.org/10.1016/j.chaos.2020.110184.

[11] A.A. Thirthar, S.J. Majeed, M.A. Alqudah, et al. Fear effect in a predator-prey model with additional food, prey refuge and harvesting on super predator, Chaos Solitons Fractals. 159 (2022), 112091. https://doi.org/10.1016/j.chaos.2022.112091.

[12] C. Maji, Impact of fear effect in a fractional-order predator-prey system incorporating constant prey refuge, Nonlinear Dyn. 107 (2021), 1329-1342. https://doi.org/10.1007/s11071-021-07031-9.

[13] D. Bhattacharjee, D. Das, S. Acharjee, et al. Two predators one prey model that integrates the effect of supplementary food resources due to one predator's kleptoparasitism under the possibility of retribution by the other predator, preprint, (2023). http://arxiv.org/abs/2305.17470.

[14] P. Majumdar, S. Debnath, B. Mondal, et al. Complex dynamics of a prey-predator interaction model with Holling type-II functional response incorporating the effect of fear on prey and non-linear predator harvesting, Rend. Circ. Mat. Palermo, II. Ser. 72 (2022), 1017-1048. https://doi.org/10.1007/s12215-021-00701-y.

[15] Didiharyono, Stability analysis of one prey two predator model with Holling type III functional response and harvesting, J. Math. Sci. 1 (2016), 50-54.

[16] R.K. Upadhyay, S.N. Raw, Complex dynamics of a three species food-chain model with Holling type IV functional response, Nonlinear Anal.: Model. Control. 16 (2011), 553-374. https://doi.org/10.15388/na.16.3.14098.

[17] A. Mondal, A.K. Pal, G.P. Samanta, Stability and bifurcation analysis of a delayed three species food chain model with Crowley-Martin response function, Appl. Appl. Math.: Int. J. 13 (2018), 8.

[18] R.K. Naji, A.T. Balasim, Dynamical behavior of a three species food chain model with Beddington-DeAngelis functional response, Chaos Solitons Fractals. 32 (2007), 1853-1866. https://doi.org/10.1016/j.chaos.2005.12.019.

[19] M. Freeze, Y. Chang, W. Feng, Analysis of dynamics in a complex food chain with ratio-dependent functional response, J. Appl. Anal. Comput. 4 (2014), 69-87. https://doi.org/10.11948/2014002.

[20] N.K. Hughes, C.J. Price, P.B. Banks, Predators are attracted to the olfactory signals of prey, PLoS ONE. 5 (2010), e13114. https://doi.org/10.1371/journal.pone.0013114.

[21] R.E. Brown, D.W. MacDonald, Social odours in mammals, Volumes 1 and 2, Clarendon Press, Oxford, UK, (1985).

[22] H. Arakawa, D.C. Blanchard, K. Arakawa, et al. Scent marking behavior as an odorant communication in mice, Neurosci. Biobehav. Rev. 32 (2008), 1236-1248. https://doi.org/10.1016/j.neubiorev.2008.05.012.

[23] Z.T. Halpin, Individual odors among mammals: origins and functions, Adv. Stud. Behav. 16 (1986), 39-70. https://doi.org/10.1016/s0065-3454(08)60187-4.

[24] N.K. Hughes, J.L. Kelley, P.B. Banks, Dangerous liaisons: the predation risks of receiving social signals, Ecol. Lett. 15 (2012), 1326-1339. https://doi.org/10.1111/j.1461-0248.2012.01856.x.

[25] M.R. Conover, Predator-prey dynamics: the role of olfaction, CRC Press, Boca Raton, (2007).

[26] I. Saavedra, L. Amo, Insectivorous birds eavesdrop on the pheromones of their prey, PLoS ONE. 13 (2018), e0190415. https://doi.org/10.1371/journal.pone.0190415.

[27] H.S. Wu, F. Zhang, L. Wu, New swarm intelligence algorithm-wolf pack algorithm, Syst. Eng. Electron. 35 (2013), 2430-2438.

[28] C. Threlfall, B. Law, P.B. Banks, Odour cues influence predation risk at artificial bat roosts in urban bushland, Biol. Lett. 9 (2013), 20121144. https://doi.org/10.1098/rsbl.2012.1144.

[29] J.P. Bytheway, C.J. Price, P.B. Banks, Deadly intentions: naïve introduced foxes show rapid attraction to odour cues of an unfamiliar native prey, Sci. Rep. 6 (2016), 30078. https://doi.org/10.1038/srep30078.

[30] P.X. Shen, Y.K. Xue, Analysis of model in a predator-prey system with refuge under the impact of odor, J. Chongqing Univ. Technol. (Nat. Sci.), 32 (2018), 205-211.

[31] W. Xu, D. Wu, J. Gao, et al. Mechanisms of stable species coexistence in food chain systems: Strength of odor disturbance and group defense, Chaos Solitons Fractals: X. 8 (2022), 100073. https://doi.org/10.1016/j.csfx.2022.100073.

[32] R.R. Lawson, D.T. Fogarty, S.R. Loss, Use of visual and olfactory sensory cues by an apex predator in deciduous forests, Can. J. Zool. 97 (2019), 488-494. https://doi.org/10.1139/cjz-2018-0134.

[33] S.E. Hygnstrom, Black bears, The Handbook: Prevention and Control of Wildlife Damage, 29, (1994).

[34] T.G. Smith, I. Stirling, Predation of harp seals, Pagophilus groenlandicus, by polar bears, Ursus maritimus, in Svalbard, Arctic, 72 (2019), 197-202. https://www.jstor.org/stable/26739928.

[35] K. Mischaikow, H. Smith, H.R. Thieme, Asymptotically autonomous semiflows: chain recurrence and Lyapunov functions, Trans. Amer. Math. Soc. 347 (1995), 1669-1685.

[36] L. Perko, Differential equations and dynamical systems, Texts in Applied Mathematics, Vol. 7, Springer, New York, (2013).

[37] B.D. Hassard, N.D. Kazarinoff, Y.H. Wan, Theory and applications of Hopf bifurcation, Cambridge University Press, Cambridge, (1981).

[38] A. Dhooge, W. Govaerts, Yu.A. Kuznetsov, et al. New features of the software MatCont for bifurcation analysis of dynamical systems, Math. Computer Model. Dyn. Syst. 14 (2008), 147-175. https://doi.org/10.1080/13873950701742754.